ELSEVIER

Surface Science 399 (1998) 135–159

surface science

Adsorption and thermal desorption on stepped surfaces

S.H. Payne, H.J. Kreuzer *

Department of Physics, Dalhousie University, Halifax, NS, Canada B3H 3J5

Received 21 February 1997; accepted for publication 9 September 1997

Abstract

A lattice gas model for the adsorption and thermal desorption on stepped surfaces is formulated with different adsorption sites on the terraces, the lower base and the upper edge of the steps and including various lateral interactions. We employ transfer matrix techniques to get the equilibrium properties, correlation functions and temperature-programmed desorption spectra. A systematic study is presented on the effect of varying terrace widths for atomic, molecular and dissociative adsorption with attractive and/or repulsive lateral interactions. We also present preliminary fits to experimental data on Xe, CO and hydrogen desorption from stepped Pt(111) surfaces. © 1998 Elsevier Science B.V.

Keywords: Growth; Models of surface kinetics; Stepped single crystal surfaces; Thermal desorption

1. Introduction

Steps, kinks and defects play an important role in the kinetics of surface processes such as adsorption, desorption and reactions [1–4]. The modification of the electronic density in the vicinity of the steps leads to: (i) different adsorption sites, i.e. different in their geometry and their binding energy from the flat terraces; (ii) different lateral interactions between particles adsorbed at the steps; and (iii) different reaction probabilities and even reaction paths. That these features are most important for heterogeneous catalysis has been known since the beginnings of surface science and has been the reason why, in addition to adsorption studies on atomically flat surfaces, great efforts have been made to understand the additional processes and reaction pathways introduced by the presence of steps and kinks on well-defined stepped surfaces as an important step towards a full comprehension of the reactivity of real catalysts.

Theoretical approaches to the kinetics at stepped surfaces have been mostly phenomenological in nature: one writes down a set of coupled rate equations with phenomenological rate constants which are fitted to experimental data. As has been shown over recent years such an approach is not even adequate for the much simpler situation of the kinetics at atomically flat surfaces, most importantly because it does not incorporate the effect of lateral interactions in the adsorbate. In this paper we will therefore extend the theory of adsorption and desorption on flat surfaces to include steps. The theory is based on nonequilibrium thermodynamics and uses lattice gas models to describe the structure of the surface and the adsorbate. Similar models have been used to describe surface diffusion on flat and stepped surfaces employing Monte Carlo techniques whereas our theory is largely

* Corresponding author. Fax: +1 902 494 5191; e-mail: kreuzer@is.dal.ca

PII S0039-6028(97)00737-1

analytical using transfer matrix techniques for the final evaluation of thermodynamic properties (adsorption isotherms, heats of adsorption, adsorption entropies, growth modes etc.) and kinetic data (TPD spectra).

In the next section we define the lattice gas model to describe the various adsorption sites on the terraces and at the steps of a stepped surface. We specify the Hamiltonian of the system by assigning different adsorption energies and vibrational properties to the various sites and introducing lateral interactions between the various adsorbed species.

To model the adsorption–desorption kinetics we will assume that fast surface diffusion (fast on the time scale of adsorption and desorption) maintains the adsorbate in quasi-equilibrium. In such situations the desorption kinetics are completely specified by the fugacity of the adsorbate and all we need is the chemical potential of the adsorbate from which we can also calculate the equilibrium properties. Frequently sticking, dissociation and reaction is enhanced by the presence of steps. This can be incorporated in our theory by assigning different sticking or dissociation probabilities to the step and terrace sites.

In Sections 3–8 we present a systematic study of adsorption and desorption at a sequence of stepped surfaces with progressively narrower terrace widths. In numerical examples we will show predominantly temperature-programmed desorption (TPD) spectra for the total desorption rates and for the partial (site) rates, and also heats of adsorption, adsorption entropies, growth curves and correlation functions. Our purpose is to illustrate the diversity and complexity that may arise in these properties, both as the terrace width is varied, with other system parameters held constant, and as lateral interactions and site binding energies are varied. Some of our examples are representative only, but others are actual attempts to fit experimental data.

In Section 3 we briefly look at adsorbates without any lateral interactions to establish a reference point for the ensuing discussion. In Section 4 we look at adsorbates with predominantly attractive interactions such as metals or rare gases, and in Section 5 we give an account of Xe adsorption on Pt(557) and Pt(112) for which experimental data are available. In Section 6 we look at molecular adsorbates with predominantly repulsive interactions, and in Section 7 we have a preliminary look at CO on two stepped Pt surfaces. In Section 8 we briefly study dissociative adsorption, such as hydrogen, on these surfaces. We close the paper with a discussion of extensions of the formalism than can and should be undertaken.

2. Lattice gas model

We assume that the surface of the solid provides localized adsorption sites which do not change in their geometric pattern as the coverage of the adsorbate increases although the energetics of course can. To define a lattice gas model we divide the surface into an array of cells each containing one adsorption site which we label with an index i (the generalization to more than one adsorption site or different adsorption states in one unit cell is straightforward and has been presented elsewhere [5,6] for flat surfaces). We allow the adsorption sites at the base (b) and on the upper edge (e) of the steps to be energetically different from those on the interior of the terraces (t). We introduce occupation numbers $n_i^{(\mathrm{t})}$, $n_i^{(\mathrm{b})}$ and $n_i^{(\mathrm{e})}$ equal to 0 or 1 depending on whether the terrace, base or edge sites, respectively, are empty or occupied. We then write the Hamiltonian of the system as

$$\begin{aligned} H = \sum_i & (E_{\mathrm{t}} n_i^{(\mathrm{t})} + E_{\mathrm{e}} n_i^{(\mathrm{e})} + E_{\mathrm{b}} n_i^{(\mathrm{b})}) + V_1^{(\mathrm{t-t})} \sum_{i,a} n_i^{(\mathrm{t})} n_{i+a}^{(\mathrm{t})} \\ & + V_1^{(\mathrm{b-b})} \sum_{i,a} n_i^{(\mathrm{b})} n_{i+a}^{(\mathrm{b})} \\ & + V_1^{(\mathrm{e-e})} \sum_{i,a} n_i^{(\mathrm{e})} n_{i+a}^{(\mathrm{e})} + V_1^{(\mathrm{e-t})} \sum_{i,a} n_i^{(\mathrm{t})} n_{i+a}^{(\mathrm{e})} \\ & + V_1^{(\mathrm{t-b})} \sum_{i,a} n_i^{(\mathrm{t})} n_{i+a}^{(\mathrm{b})} + V_{1\mathrm{s}}^{(\mathrm{b-e})} \sum_{i,a} n_i^{(\mathrm{e})} n_{i+a}^{(\mathrm{b})} \\ & + V_2^{(\mathrm{t-t})} \sum_{i,a} n_i^{(\mathrm{t})} n_{i+a}^{(\mathrm{t})} + \ldots \end{aligned} \tag{1}$$

The first term in Eq. (1) accounts for the energy gain due to the interaction with the surface. The single particle energies are given (on the terraces, as an example) by expressions like [5]

$$E_{\mathrm{t}} = -V_{\mathrm{t}} - k_{\mathrm{B}} T \ln(q_3^{(\mathrm{t})} z_{\mathrm{vr}}^{(\mathrm{t})} / Z_{\mathrm{vr}}), \tag{2}$$

where V_t is the depth of the adsorption potential of a (terrace) site, $q_3^{(t)}$ is the single particle partition function of a particle adsorbed in this site accounting for its vibrations perpendicular and parallel to the surface. Z_{vr} is the partition function for molecular vibrations and rotations in the gas phase, and z_{vr} accounts for hindered vibrations and rotations on the surface. The remaining terms in Eq. (1), pre-multiplied by $V_1^{(i-j)}$, account for the lateral interaction between two particles adsorbed on nearest neighbor sites on a terrace except for $V_{1s}^{(b-e)}$ which couples sites across the step. Similar terms with V_2 account for next nearest neighbor interactions.

Our examples will be for the fcc-$n(111)\times(100)$ surfaces which have a (111) terrace width of n (rows of) substrate atoms. However, this need not be the number of adsorption sites which enters the construction of the lattice gas. E.g. in a monolayer of Xe on Pt(557) (with $n=6$ Pt atoms per terrace) there are only five rows of three-fold hollow sites per terrace. We will therefore in the following use a classification according to the number m of rows per terrace in the monolayer adsorbate and denote these as m-surfaces. In addition we distinguish between adsorbates with the same lattice structure as the substrate, e.g. for on-top adsorption (which we will call the on-top model) and those with the $(\sqrt{3}\times\sqrt{3})$R30° superstructure (which we will call the rotated model). Fig. 1a shows an example of the rotated model with nearest and next nearest neighbor interactions for a terrace of width 5 adsorption sites ($m=5$), i.e. on a $7(111)\times(100)$ substrate with 7 substrate atoms per terrace. Fig. 1b shows the situation for $m=3$; there are two nearest neighbor bonds connecting the b- and e-sites, $V_1^{(e-b)}$ on the terrace and $V_{1s}^{(b-e)}$ across the step. For comparison we sketch in Fig. 1c the on-top model for $m=4$ showing that the number and direction of nearest and next nearest neighbor couplings are different from those in the $m=4$ rotated model.

To model the adsorption–desorption kinetics we will restrict ourselves to systems for which surface diffusion is fast enough, on the time scale of adsorption and desorption, to maintain the adsorbate in quasi-equilibrium. This constraint has been used successfully to model the desorption kinetics on flat surfaces, and we expect it to apply to the

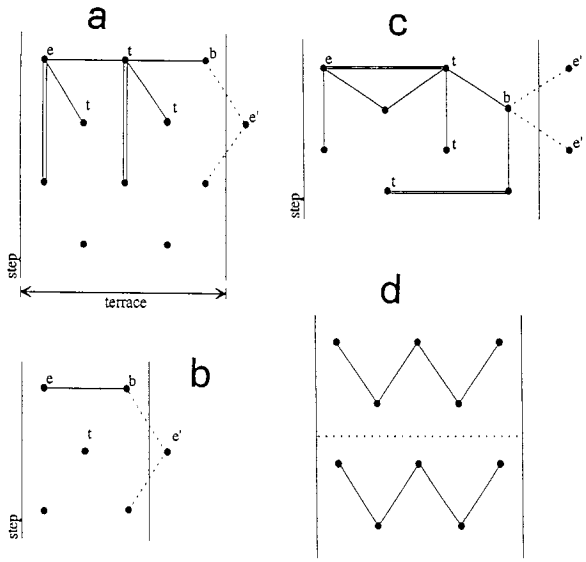

Fig. 1. Schematics of adsorption sites and lateral interactions on stepped surfaces. Single lines: nearest neighbor interactions, e.g. along the top line of (a) $V_1^{(e-t)}$ and $V_1^{(t-b)}$; double lines: next nearest neighbor interactions, e.g. along the top line of (c) $V_2^{(e-t)}$; dashed lines: interaction $V_{1s}^{(b-e)}$ across the steps. (a) The rotated adsorbate structure for $m=5$, (b) for $m=3$, (c) the on-top structure with $m=4$. (d) Shows the two "*columns*" of connected sites used in the transfer matrix construction for $m=5$.

terraces of stepped surfaces as well. Diffusion across the steps may be limited by the presence of more tightly bound particles in which case the individual terraces may be decoupled. To what extent this occurs depends on the nature of the lateral interactions and the site binding energies [7–9]. Systems in quasi-equilibrium are completely characterized by the coverage, θ, and we get the adsorption and desorption rates, for nondissociative adsorption as an example, [5,10,11]

$$\frac{d\theta}{dt} = R_{ad} - R_{des}, \tag{3}$$

$$R_{ad} = S(\theta,T)a_s \frac{\lambda}{h} P, \tag{4}$$

$$R_{des} = S(\theta,T)a_s \frac{k_B T}{h\lambda^2 q_3^{(t)}} \frac{Z_{vr}}{z_{vr}^{(t)}} \times e^{-V_t/k_B T} \frac{\theta}{1-\theta} e^{\mu_i(\theta,T)/k_B T}, \tag{5}$$

with a_s the area of an adsorption site, $S(\theta,T)$ is the sticking coefficient and P the instantaneous pressure. The dependence of the desorption rate on the binding differences, differences in site partition functions and the lateral interaction energies between t, e and b sites, is accounted for in the interaction part of the chemical potential, $\mu_i(\theta,T)$, which we must calculate from the Hamiltonian (Eq. (1)). To calculate the coverage and temperature dependence of μ_i we employ the transfer matrix method [11]. The transfer matrix is constructed for interactions between two adjacent "*columns*" of m adsorption sites perpendicular to the step edge, Fig. 1d, with the 2^m occupation states of these sites indexing the matrix. With the constraint of periodicity in this direction (i.e. the b-site at the end of the "*column*" may couple to the e-site on the terrace above), two "*columns*" incorporate the interactions in Eq. (1). Unlike that for the (homogeneous) fcc(111) surface, the transfer matrix can no longer be block diagonalized. This limits the width of the terrace (m) that one can study. As discussed elsewhere [12–16] the leading eigenvalue of the transfer matrix corresponds to the grand partition function and its corresponding eigenvector determines the probabilities of the allowed states of the "*column*". In particular, the partial coverages for the t-, e- and b-sites are available as a function of coverage, i.e.

$$\theta=\theta_e+\theta_t+\theta_b=[\langle n_i^{(e)}\rangle+(m-2)\langle n_i^{(t)}\rangle+\langle n_i^{(b)}\rangle]/m. \tag{6}$$

To complete the theory we need to specify the coverage dependence of the sticking coefficient. It is a measure for the efficiency of energy transfer in adsorption and desorption. As such it cannot be obtained from thermodynamic arguments but must be calculated from a microscopic theory or taken from experiment. For a noninteracting adsorbate the sticking coefficient decreases linearly (quadratically) on a flat surface for nondissociative (dissociative into two fragments) adsorption. For a stepped surface this is still true for the dependence on the partial coverages, i.e. one writes for direct nondissociative adsorption

$$\begin{aligned}S(\theta,T)a_s=&S_e(T)(1-\langle n_i^{(e)}\rangle)a_{se}\\&+S_t(T)(1-\langle n_i^{(t)}\rangle)a_{st}\\&+S_b(T)(1-\langle n_i^{(b)}\rangle)a_{sb}.\end{aligned} \tag{7}$$

Here we also allowed for the areas of the different adsorption sites to be different. Even in this simple form one can account for preferential adsorption at steps by choosing S_t much smaller than S_e or S_b. To recover the simple $1-\theta$ dependence the products of initial sticking and site areas are in the ratio of the partial coverages. Sticking is generally effected by the lateral interactions in the adsorbate. This leads often to a constant sticking coefficient in adsorbates with lateral attractions and to rapidly decreasing sticking for strong lateral repulsions. Once precursors come into play the coverage and temperature dependence of sticking is further modified. The effect of lateral interactions on precursor-mediated sticking has recently been studied for adsorption on flat surfaces on the basis of a kinetic lattice gas model [17]. It essentially replaces the occupation probabilities in Eq. (7) by correlation functions induced by lateral interactions leading to a great variety of coverage and temperature dependent sticking coefficients. Although this can readily be adopted to stepped surfaces we will for the numerical examples in this paper choose appropriate sticking coefficients phenomenologically.

In our numerical examples we will frequently show and discuss the isosteric heat of adsorption, i.e. the enthalpy change per particle adsorbed

$$Q_{iso}=k_B T^2\,\partial\ln P/\partial T|_\theta=-\partial(\beta\mu)/\partial\beta|_\theta, \tag{8}$$

and the corresponding differential entropy

$$\Delta\bar{S}_{ads}=\bar{S}_{adsorbate}-\bar{S}_{gas}=-k_B\ln(P/P_0)-Q_{iso}/T. \tag{9}$$

In the interpretation of experimental data one may write the desorption rate in the Arrhenius parametrization, assuming a desorption order x

$$\frac{d\theta}{dt}|_{des}=\nu_{eff}(\theta)\theta^x\exp(-E_d(\theta)/k_B T), \tag{10}$$

and extract the effective prefactor, $\nu_{eff}(\theta)$, and the desorption energy, $E_d(\theta)$, from an isosteric analysis

of the TPD spectra. Note that for systems in quasi-equilibrium the desorption energy is an average of the heat of adsorption over the temperature range of desorption and that the effective prefactor is related to the differential entropy, $\nu_{\mathrm{eff}} \propto \exp(-\Delta S/k_{\mathrm{B}})$ (again averaged over the desorption range).

3. Atomic adsorption with zero/weak interactions

We use the lattice gas model defined by the Hamiltonian (Eq. (1)) to explain the thermodynamic and kinetic properties of dissociative and nondissociative adsorption on a series of stepped surfaces with decreasing terrace widths. Although our examples will be for the fcc-$n(111)\times(100)$ surfaces, we do not expect qualitatively different results for other surfaces. The majority of the examples will be for an adsorbate with the $(\sqrt{3}\times\sqrt{3})\mathrm{R}30^{\circ}$ structure. We limit our study to terrace widths $m=2$–7 because this encompasses most of the interesting experimental studies.

The calculations proceed as follows: Once the adsorption sites, binding and interaction energies are specified, the transfer matrix is constructed as discussed above. From the grand partition function we determine the chemical potential, $\mu_i(\theta,T)$, self-consistently as a function of coverage and temperature which allows us to determine equilibrium properties (isobars, the heat of adsorption, entropy changes), and the desorption kinetics.

First we look at an atomic adsorbate in which lateral interactions can be neglected altogether. This will serve as a reference for the effects of significant lateral interactions. Recall that adsorption on a flat surface such as a fcc(111) surface for the situation where the surface provides only one type of adsorption site is simple: (i) the equilibrium properties are given by the Langmuir isotherm, (ii) the heat of adsorption is constant and equal to the binding energy of a single atom to the surface (plus small corrections from the vibrational degrees of freedom), (iii) the sticking coefficient decreases linearly with coverage due to site exclusion only, and (iv) desorption is first-order. This picture maintains for a stepped surface in which the binding energy at the steps is so much larger than on the terrace that the corresponding TPD peaks do not overlap. If there are n_{t} and n_{s} adsorption sites per unit cell on the terrace and on the steps, respectively, then the heat of adsorption drops around a coverage $n_{\mathrm{s}}/(n_{\mathrm{s}}+n_{\mathrm{t}})$ from its value at the steps to that on the terrace. Up to that initial coverage desorption occurs in a high temperature TPD peak from the steps only, and at full coverage the areas under the (separate) TPD peaks are in the ratio $n_{\mathrm{s}}/n_{\mathrm{t}}$.

The kinetics become interesting when the binding characteristics are such that desorption from terraces and steps compete. In Fig. 2 we present TPD data for an adsorbate on various stepped surfaces neglecting lateral interactions and choosing a sticking coefficient due to site exclusion only, as appropriate for a noninteracting adsorbate. All vibrational frequencies are taken to be equal, for simplicity (though this is rarely the case in nature). We have taken the binding energy at the base of the step, V_{b}, to be close to that on the terrace, V_{t}, but much lower than that on the upper edge of the step, V_{e}. This is the case for the systems studied here but not for all. As a result the desorption peak from the upper edge is well separated from the overlapping peaks from the bottom of the steps and from the terraces, Fig. 2a. The main peaks, due to desorption from the t-sites, are all around 520 K and are quite symmetric indicating first-order kinetics. Although this would also be the case for desorption from the minority edge sites if they were not kept in quasi-equilibrium with the b- and t-sites by fast surface diffusion, their desorption peaks shift considerably to lower temperature for increasing initial coverage. This is due to the fact that at the elevated temperatures of desorption from the e-sites the t-sites are empty, and the b-sites nearly so, and desorption can proceed in two steps, i.e. a fast repopulation of t- and b-sites followed by desorption from there. That desorption from the terrace and step sites is not altogether independent from each other despite the fact that there are no lateral interactions in action, we can see from the corresponding partial rates, as depicted in Fig. 2b. Here and elsewhere we have rescaled these rates as follows: the partial rate from the t-sites is reproduced on the scale of

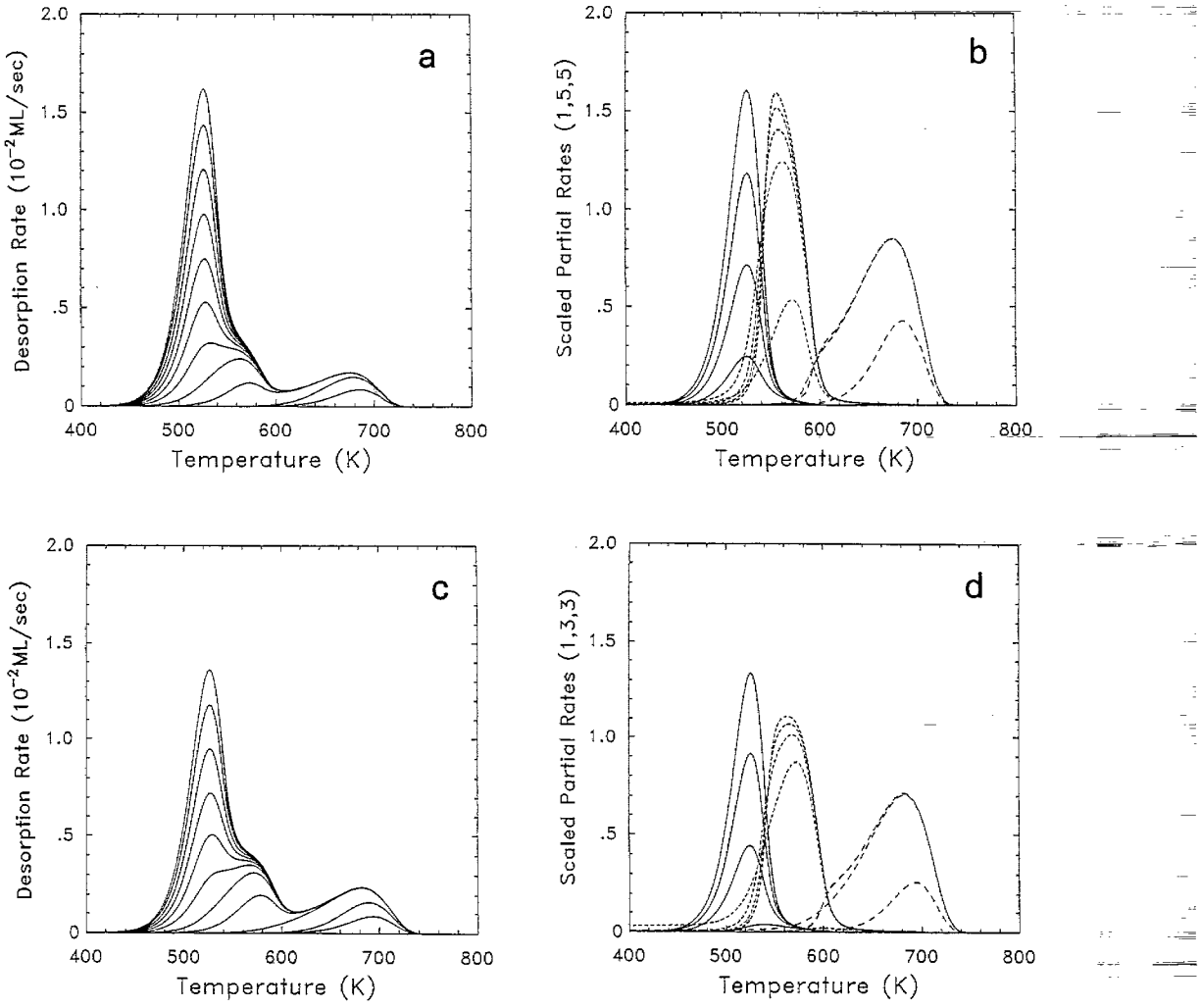

Fig. 2. TPD spectra for a noninteracting adsorbate on various stepped surfaces with the rotated adsorbate structure. Left column: total desorption rates. Right column: partial rates (for every other initial coverage only) from t-sites (solid lines), b-sites (dotted) and e-sites (dashed). Initial coverages 0.05, 0.1, 0.2, 0.3,..., 0.9, 0.98 and heating rate 1 K s^{-1}. The factors by which the partial rates are scaled are indicated in order on the axis label. Sticking coefficient $S(\theta)=1-\theta$. Common parameters: $V_t=1.46$ eV, $V_b=1.7$ eV, $V_e=2.0$ eV, $\nu_z=\nu_x=\nu_y=10^{12}$ s^{-1} for all species, $a_s=16$ Å^2, $m=28$ amu. (a,b) 7-surface, (c,d) 5-surface, (e,f) 3-surface, (g,h) 2-surface.

Fig. 2a but those of the e- and b-sites are enhanced, for clarity, by a factor equal to the number of terrace sites, $m-2$. Because fast surface diffusion is assumed to maintain quasi-equilibrium during desorption there is instant re-distribution of particles among the adsorption sites even before significant desorption takes place. Once the temperature is high enough to activate desorption from the (slightly stronger bound) b-sites at the bottom of the steps the latter sets in, but not with the long rising edge seen at lower temperature for desorption from the terraces. The total and partial rates for $m=5, 3, 2$ are shown in Fig. 2c–h. Clearly, desorption from the 7- and 5-surfaces has more in common than desorption from the 3- and 2-surfaces. Since on the m-site surface $1/m$ of a monolayer desorb from the e-sites under the high temperature peak, on the surface with e- and

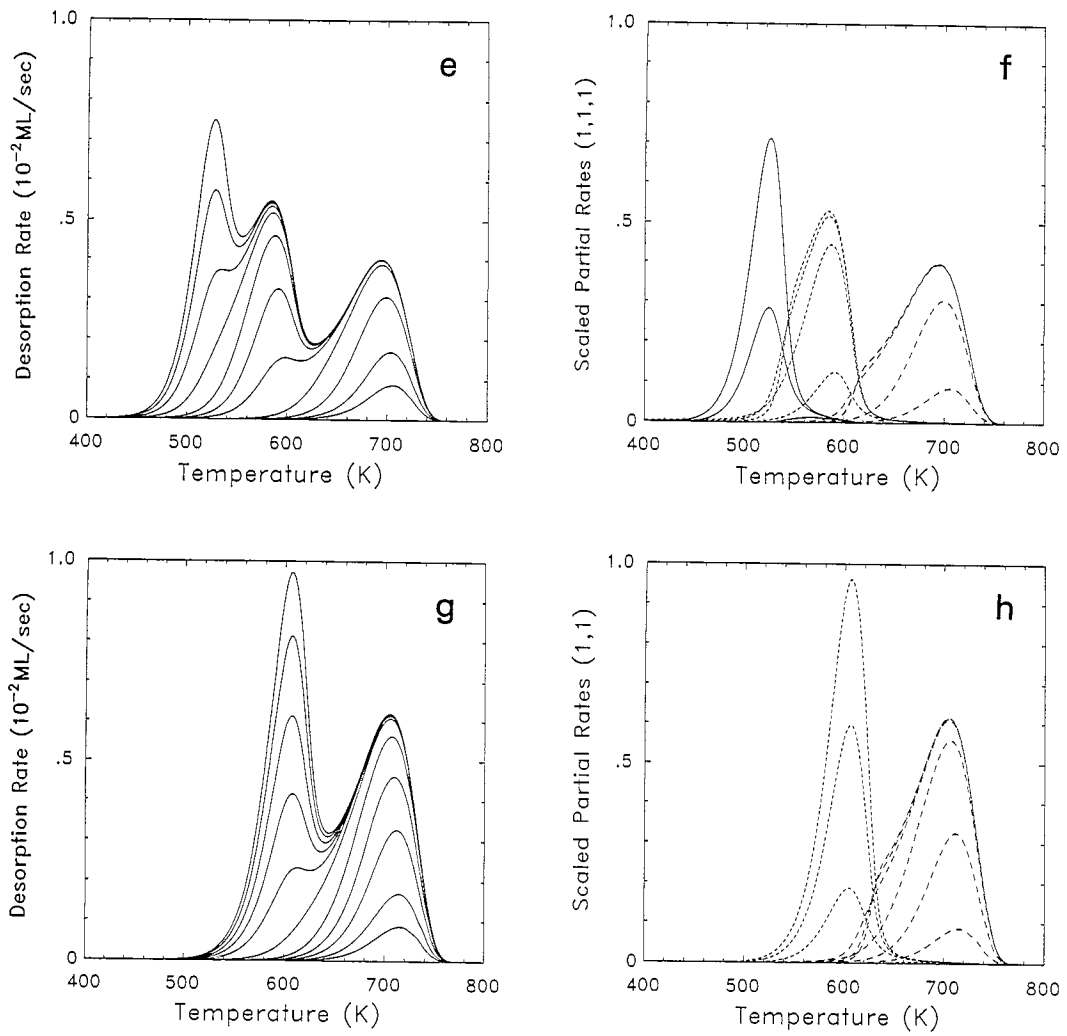

Fig. 2 (*continued*)

b-sites only, half of a monolayer desorbs from either. As the asymmetry of the partial rates of Fig. 2h indicates clearly, it would be wrong to represent the double-humped TPD spectra by a superposition of two independent desorption peaks (as it is often done in the evaluation of experimental data) because desorption from the more strongly bound e-sites is delayed as long as there is a significant population of the more weakly bound b-sites remaining. We elaborate this point further with an analytical example in Appendix A.

In Fig. 3 we show a series of examples for which the binding energies on the terrace and at the step ($V_e \simeq V_b$) are only marginally different (by about 10%). An inspection of the partial rates shows that the TPD spectra of the step sites are, again, not those of a noninteracting adsorbate, and the desorption from the terraces is not first-order. In fact, these single peak spectra look very much like those originating from an adsorbate with weak lateral repulsions which, of course, they are not. The difference shows up in the coverage dependence of the heat of adsorption (or desorption energy). For an adsorbate with weak repulsion, V_1, the heat of adsorption decreases linearly with coverage whereas on the stepped surfaces the heat

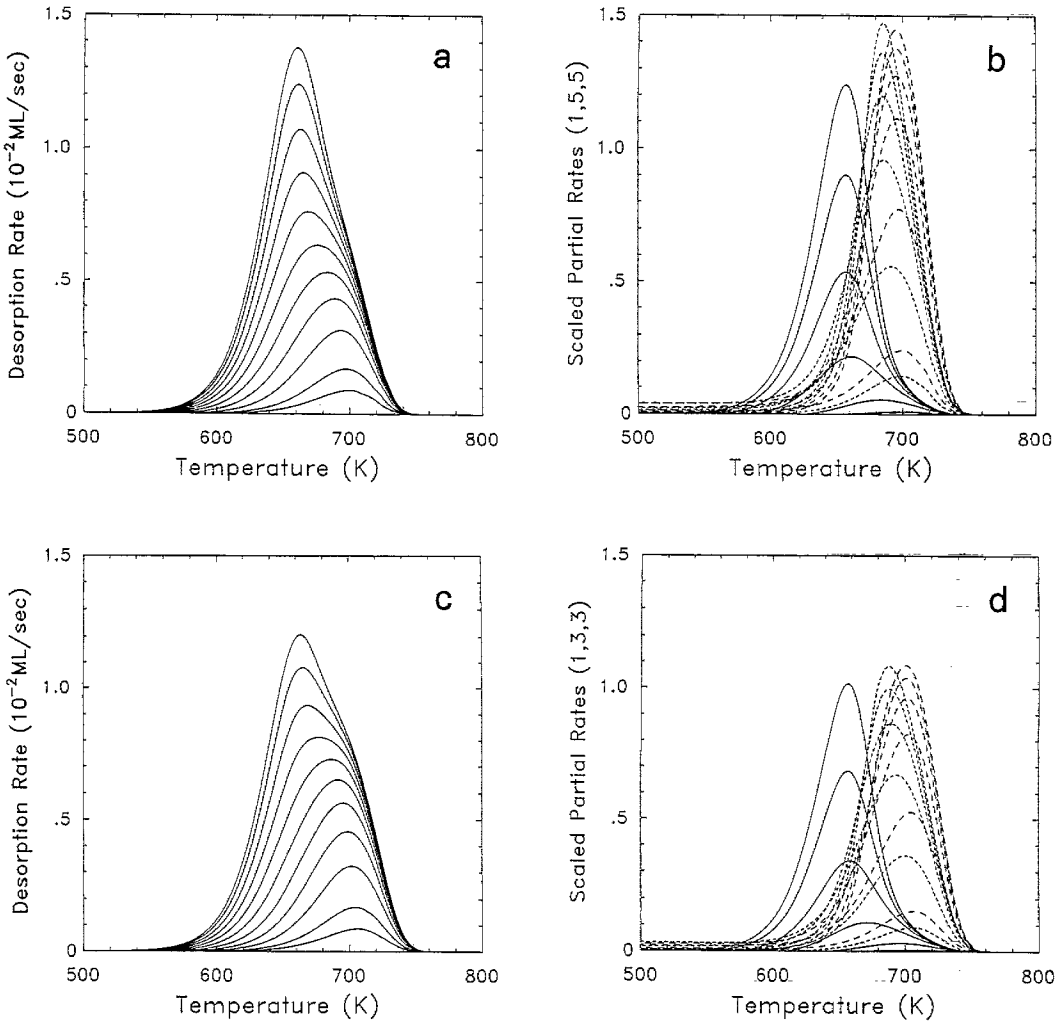

Fig. 3. TPD spectra for a noninteracting adsorbate on various stepped surfaces with the rotated adsorbate structure. All parameters (and geometries) as in Fig. 2 except $V_t = 1.8$ eV, $V_b = 1.96$ eV ($V_e = 2.0$ eV).

of adsorption shows distinct drops at the saturation coverages of the e- and b-sites and remains constant for larger coverages.

4. Atomic adsorption with mainly attractive interactions

We next study the effect of lateral interactions and concentrate in this section on adsorbates that have mainly attractive interactions on the equivalent flat surface, in our case fcc(111). Examples are rare gases and metals on transition and noble metals. Let us further assume that on the flat surface the lateral attraction is so strong that desorption proceeds below the critical temperature, i.e. out of the *co*-existing dilute and condensed 2D phases on the surface implying that desorption is zero-order (for constant sticking) except for coverages close to zero and one. The modification of the electron density at steps has two effects: (i) it (usually) increases the binding energy of a single atom both at the bottom and on the edge of the steps (CO on the steps of Ni(111), however,

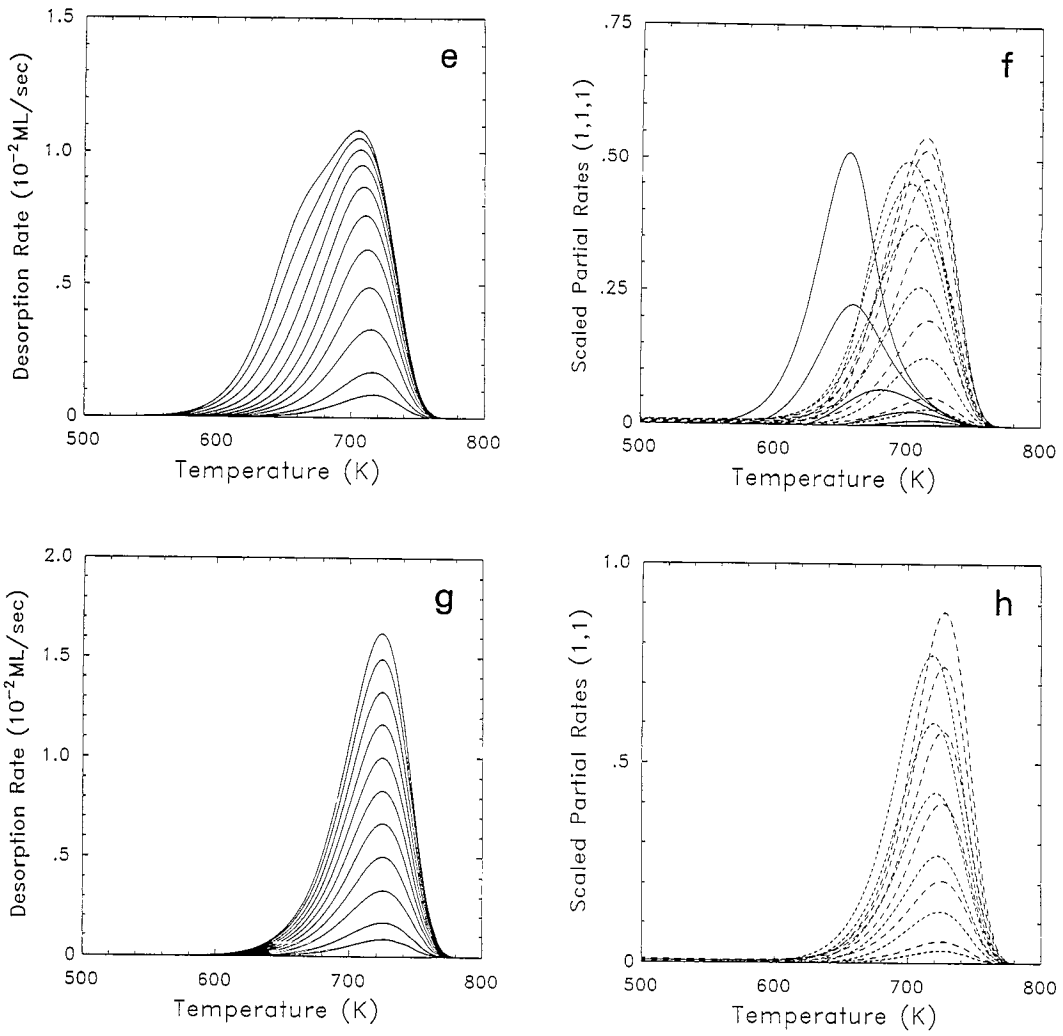

Fig. 3 (*continued*)

provides a counter example [18]); and (ii) it modifies the lateral interactions between particles adsorbed along the steps and to their neighbors on the terraces. The latter may actually change from attractive on the terraces to repulsive along the steps, as it does e.g. for xenon on stepped Pt(111) surfaces, but the gain in binding energy at the steps is usually large enough to lead to the decoration of the steps before adsorption proceeds to the terraces.

If there is no coupling across the steps then the terraces can be modeled as independent systems of finite width. This implies that the discontinuities of thermodynamic properties at the phase transition in the corresponding infinite system (flat surface) are smoothed. In particular, there is no sharp phase boundary and, correspondingly, there is no coverage regime where the chemical potential is strictly constant. The critical properties of such surfaces with large step widths have been studied by Monte Carlo and transfer matrix techniques [19–22].

For our example we have chosen all lateral interactions to be of the same strength and such that on the fcc(111) surface desorption is predominantly out of the co-existence region. The common

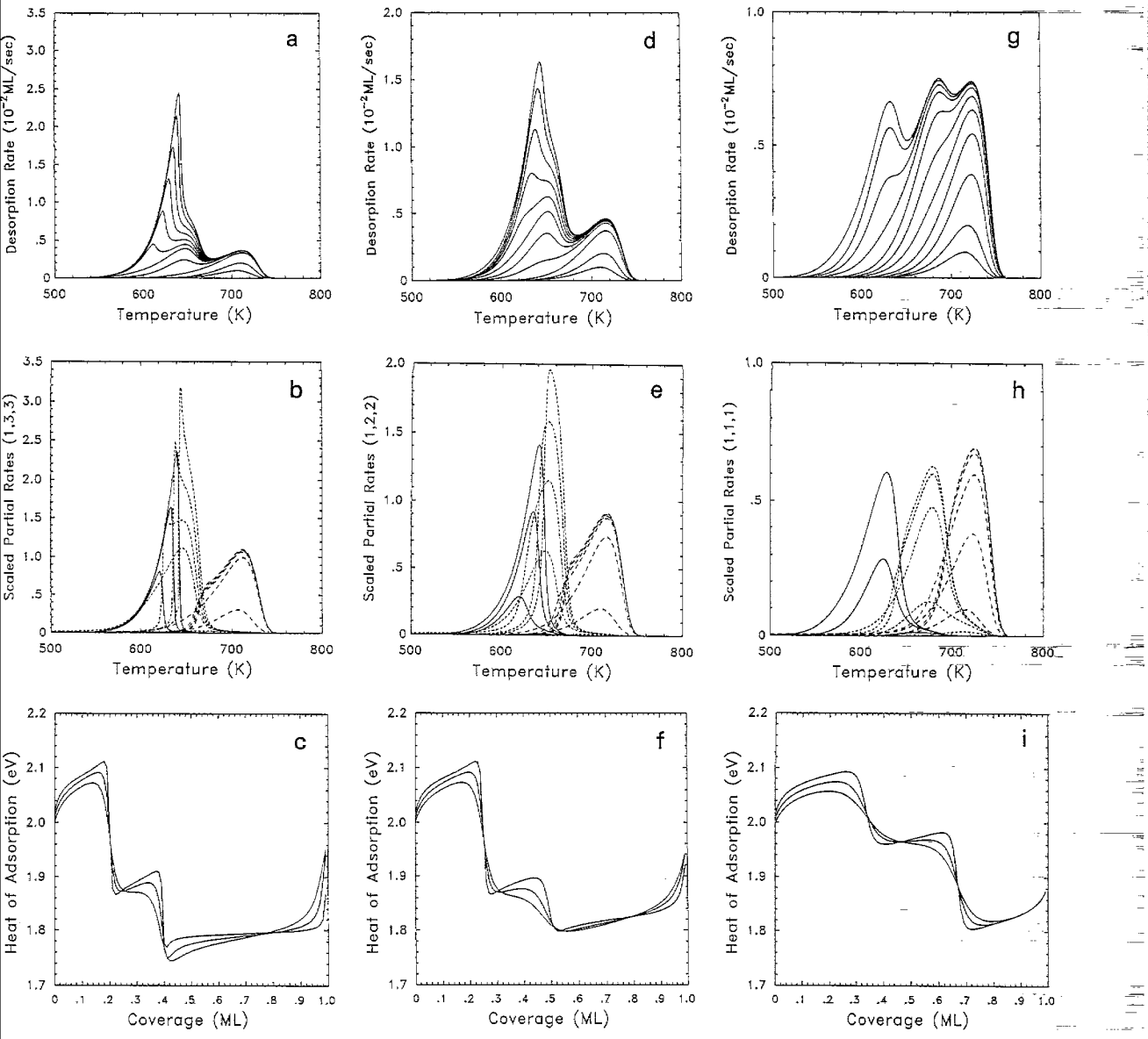

Fig. 4. TPD spectra and heat of adsorption (for temperatures 500 K, 625 K, 750 K spanning the desorption range) for an adsorbate with lateral attractions of −0.076 eV between all nearest and next nearest neighbors on various stepped surfaces with sticking coefficient $S=1$, other data as in Fig. 2. (a–c) 5-surface, (d–f) 4-surface, (g–i) 3-surface.

leading edge, indicative of zero-order desorption, essentially remains for the main peak from the 5-surface as seen in Fig. 4a. Because a lateral attraction narrows desorption peaks, what was a broad low temperature peak due to desorption from (mainly) the t-sites and a shoulder from the slightly more strongly bound b-sites (Fig. 2a) now, in the presence of lateral attraction, shows up as two distinct (and narrower) peaks. Because the subsets of e- and b-sites are one-dimensional there can be no co-existence and thus no zero-order desorption feature for these peaks. Also the high

temperature peak from the e-sites no longer shifts to lower temperatures for increasing initial coverage but to higher temperature because, with more particles adsorbed, more energy in lateral attraction is gained which has to be overcome in desorption. This is also clearly displayed in the partial rates in Fig. 4b. The additional spike in the rising edge of the partial rates from the b-sites is due to the delay in desorption as long as the terrace sites are energetically more favored. The zero-order desorption region is evident in Fig. 4c as an essentially constant heat of adsorption at lowest temperature (500 K) for $\theta > 2/5$. The sharp rise as the coverage drops below 2/5 is due to the larger binding energy for the b-sites and at 1/5 due to the e-sites. The slopes in the heat of adsorption in the coverage regimes between these rises are due to the lateral attraction between the e- and the b-sites, $V_2^{(e-e)}$ and $V_2^{(b-b)}$, respectively. We note in passing that the common leading edge for the 5-site surface pertains even if these latter second neighbor interactions are switched off. However, it disappears when we switch off $V_2^{(t-t)}$, but is still observed for the wider 7-surface.

We pointed out above that in some systems such as Xe on the stepped Pt surfaces, the lateral interactions along the steps can be repulsive. As long as desorption from these steps does not interfere with desorption from the terraces the common leading edge in TPD remains.

As we move to the surfaces with narrower terraces, Figs. 4d–i, the common leading edge completely disappears. Although we have kept the same lateral attraction between all sites the binding energy differences between the various sites destroy coexistence at the same temperature, i.e. the surface heterogeneity lowers the "*critical*" temperature of the adsorbate, in these examples actually below the temperature range of desorption. Again, this is evident from the finite slope of the heat of adsorption in the range of terrace coverage. If we had chosen an overall binding energy for the adsorbate such that at this heating rate desorption would occur in the range 300 to 500 K we would see the common leading edge on the 4-surface but no longer on the 3-surface. The smoothing of the thermodynamic singularities as a result of narrowing terrace widths will also appear in adsorption isotherms as has been observed experimentally for Xe on Cu(610) [23]. We summarize: the disappearance of a common leading edge as one goes to a surface with narrower terraces (but of the same orientation) is not necessarily due to a reduction of the lateral attraction on the terraces but can be the simple result of the energetic heterogeneity of the surface. Terrace widths as small as seven adsorbate rows can still exhibit the zero-order desorption feature (within experimental accuracy) attributed to homogeneous surfaces.

5. Xe adsorption on stepped Pt surfaces

As a specific example of some of the aspects discussed above we look at Xe adsorption and desorption on stepped Pt surfaces. As Rettner et al. [24] have shown defects on flat surfaces may influence desorption data significantly. The role of steps was systematically investigated by Siddiqui et al. by comparison of thermal desorption from Pt(111), Pt(112) and Pt(557) surfaces [25]. On the close-packed (111) surface a desorption maximum is found at 93 K upshifting with increasing coverage indicating an attractive lateral Xe–Xe interaction on the flat platinum terrace. On the stepped ((100) microfacets) surfaces they found an additional high temperature desorption peak with an adsorption energy downshifting with coverage, interpreted as due to repulsive Xe–Xe interactions along the steps.

In a recent study of xenon thermal desorption from flat Pt(111) as well as from stepped Pt(997) surfaces high-resolution TPD spectra were simulated with the present lattice gas model which included different energetics for terrace and step sites as well as different lateral interactions between xenon atoms in five adsorption rows [26]. We will now extend these models to the lower index surfaces studied by Siddiqui et al. [25]. We assume the same binding energy, frequencies and lateral attraction for the t-sites as were used in the fit to the TPD data on Pt(111). For the e- and b-sites we take the parameters obtained from the fit to the Pt(997) surface [26] so that our fit to the lower index surfaces of Siddiqui et al. [25] is parameter-free.

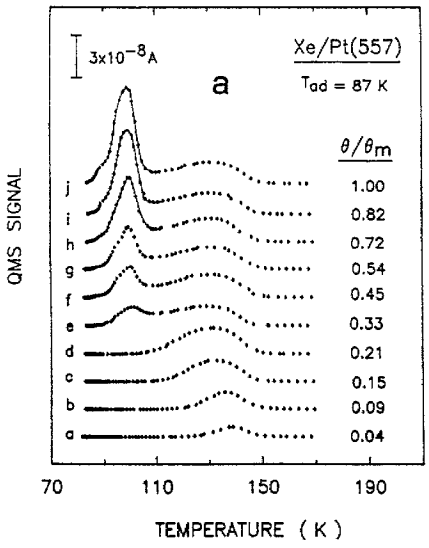
3x10⁻⁸A
Xe/Pt(557)
a
Tad = 87 K
θ/θm
j 1.00
i 0.82
h 0.72
g 0.54
f 0.45
e 0.33
d 0.21
c 0.15
b 0.09
a 0.04
QMS SIGNAL
70 110 150 190
TEMPERATURE (K)

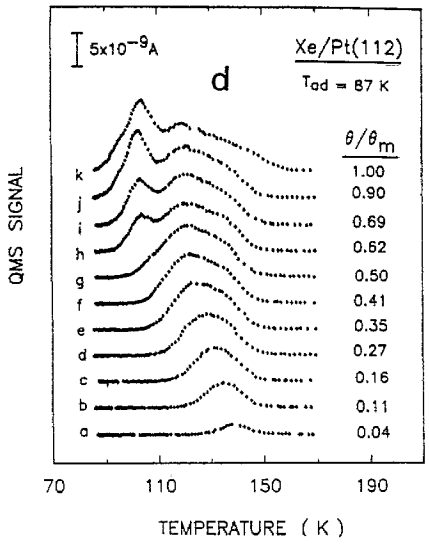
5x10⁻⁹A
Xe/Pt(112)
d
Tad = 87 K
θ/θm
k 1.00
j 0.90
i 0.69
h 0.62
g 0.50
f 0.41
e 0.35
d 0.27
c 0.16
b 0.11
a 0.04
QMS SIGNAL
70 110 150 190
TEMPERATURE (K)

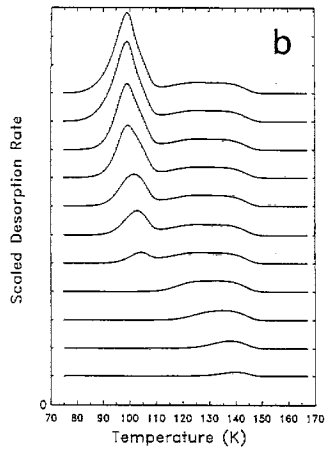
b
Scaled Desorption Rate
0
70 80 90 100 110 120 130 140 150 160 170
Temperature (K)

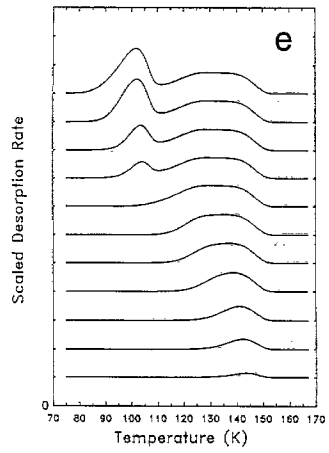
e
Scaled Desorption Rate
0
70 80 90 100 110 120 130 140 150 160 170
Temperature (K)

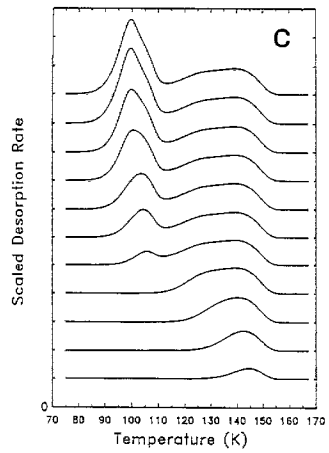
c
Scaled Desorption Rate
0
70 80 90 100 110 120 130 140 150 160 170
Temperature (K)

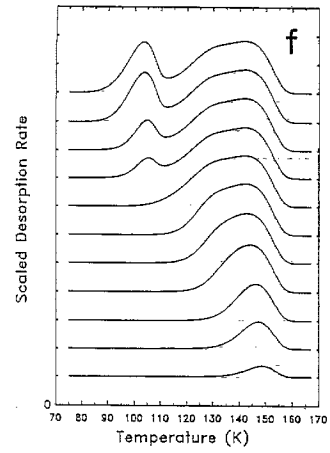
f
Scaled Desorption Rate
0
70 80 90 100 110 120 130 140 150 160 170
Temperature (K)

Although Siddiqui et al. favor an adsorption geometry with five rows per terrace, the more recent work by Widdra et al., showing that there are five rows on Pt(997), suggests fewer adsorption sites on the narrower terraces of Pt(557). We get a good fit to the data, Fig. 5a, if we assume four adsorption rows, $m=4$, i.e. excluding a row next to the e-sites. In Fig. 5b we show theoretical TPD spectra for a constant heating rate of 1 K s^{-1} which, compared to the experimental data (points), does not have enough weight in the high temperature peaks. However, Siddiqui et al.'s TPD data were generated with an increasing heating rate between 0.5 K s^{-1} at 90 K and 3 K s^{-1} at 150 K. With this heating rate we get Fig. 5c. The peak height ratios are now in good agreement, and so are the trends in the peak positions, namely that the main (terrace) peak stays more or less fixed whereas the high temperature step peak first shifts to lower temperatures with increasing initial coverages and then slightly back to higher temperatures. Overall, the theoretical peaks have shifted to slightly higher temperatures by about 4 K which, however, might be within the experimental accuracy of the temperature measurement. It could be compensated for by a reduction of the binding energies of the t-, b- and e-sites by 2%. We stress: this fit does not adjust any parameters but uses those deduced for Pt(997) except that we changed the number of adsorption rows from five on Pt(997) to four on Pt(557).

Turning to the Pt(112) surface, Figs. 5d–f, the same model parameters give a reasonable account of the experimental data. Obviously the binding energies for the e-sites are too high and for b-sites too low. Without any terrace sites left on the (112) surface one would indeed expect that the b- and e-sites become more similar. However, there is some uncertainty about the heating rate so that quantitative conclusions cannot be drawn.

6. Molecular adsorption with repulsive interactions

Lateral repulsions in an adsorbate on a flat surface induce ordered structures below the corresponding order–disorder temperatures. In the presence of steps some of these structures may only appear at much lower temperatures or be suppressed altogether, and new ones may appear. Whenever desorption occurs below and around the order–disorder temperature these structures produce additional peaks and interesting features in the TPD spectra.

For reference we show TPD spectra, heat of adsorption and differential entropy for nearest neighbor repulsion, typical of molecularly adsorbed species, e.g. CO, on a fcc(111) surface, see Figs. 6a–c. Below the order–disorder temperature $T_o \simeq 0.35 V_1^{(t-t)}/k_B$, $(\sqrt{3}\times\sqrt{3})R30°$ structures are maximal at coverages $\theta=1/3$ and 2/3. This results (at low temperatures) in sudden drops in the heat of adsorption at these coverages by amounts of $3V_1^{(t-t)}$ (and valleys in TPD) because an additional particle adsorbed into the $(\sqrt{3}\times\sqrt{3})$ structure will experience the repulsion from three neighbors. In the differential entropy the continuous decrease from coverage zero to 1/3 signals the increased order as more and more particles adsorb until the ordered structure is complete. Above $\theta=1/3$ additional particles can adsorb on an empty sublattice randomly with order increasing again until $\theta=2/3$ is reached. The process repeats on a third sublattice to a full monolayer. We have used a linearly decreasing sticking coefficient but one should remember that molecular adsorbates with strong lateral repulsions usually have sticking coefficients that drop off to zero much faster than that [11,27]. A discussion of the secondary features in the TPD spectra can be found in Refs. [11,16].

We now contrast this case of homogeneous

Fig. 5. TPD spectra for Xe on Pt(557) and Pt(112). (a) Experiment for Pt(557), (b) $m=4$ theory with heating rate 1 K s^{-1} and (c) with the experimental variable heating rate. Initial coverages as indicated. Scale in (b,c) is 0.0217 ML per division. (d–f) $m=2$ for Pt(112). Parameters: $V_t=0.264$ eV, $V_b=0.287$ eV, $V_e=0.398$ eV, $\nu_2^{(t,b,e)}=9.0\times10^{11}$ s^{-1}, $\nu_x^{(t,b,e)}=\nu_y^{(t,b,e)}=3\times10^{11}$ s^{-1}, $V_1^{(e-t)}=-0.004$ eV, $V_1^{(t-t)}=-0.011$ eV, $V_1^{(t-b)}=-0.004$ eV, $V_2^{(e-e)}=0.016$ eV, $V_{1s}^{(b-e)}=V_2^{(t-t)}=V_2^{(b-b)}=0$. Experimental data reproduced from Ref. [25].

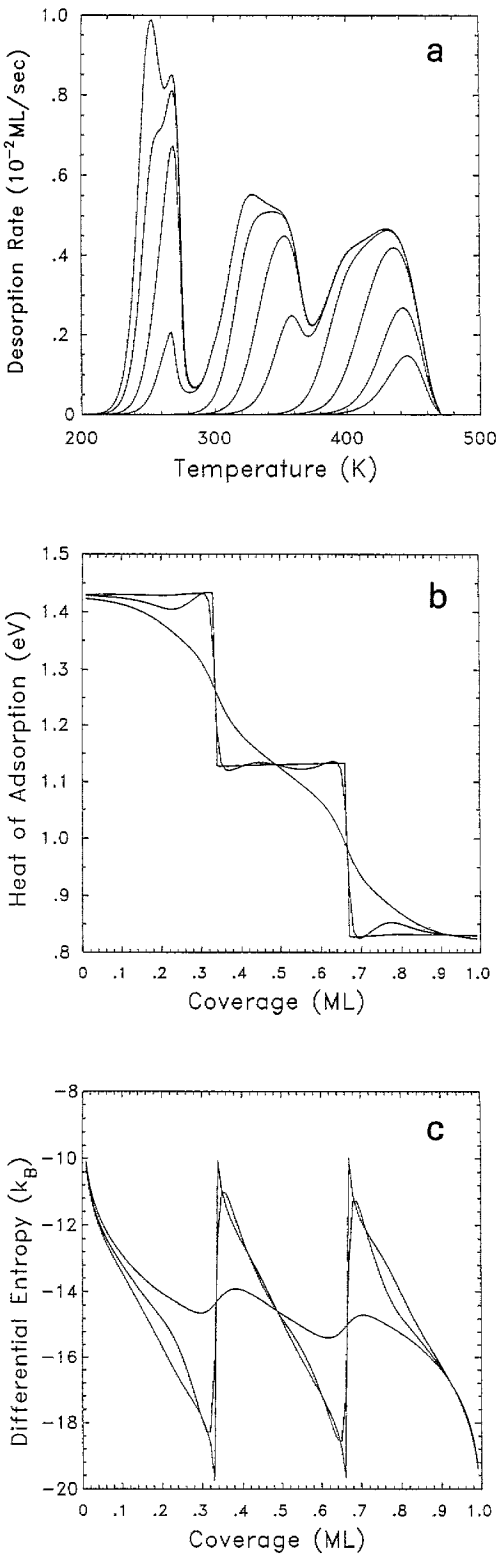

adsorption on an infinite hexagonal lattice to that on a six-row terrace ($V_e = V_t = V_b$, $V_1^{(e-t)} = V_1^{(t-t)} = V_1^{(t-b)}$, $V_2^{(i-j)} = 0$) with no coupling between terraces ($V_{ls}^{(b-e)} = 0$) nor mass transfer between them, due to a high diffusion barrier. In Fig. 7 we show adsorption–desorption data for this surface. Although we again get a three-peaked TPD spectra as depicted in Fig. 7a, the weights of the peaks differ and originate from the fact that the sites at the boundaries of the terrace see fewer neighbors resulting in a higher desorption energy as reflected in the partial rates, Fig. 7b, and partial coverages, Fig. 7c. However, the adsorption process is more complicated than the TPD spectra imply as is revealed by the growth curves, i.e. the partial coverages (presented in the figures as average site occupations) as a function of total coverage for fixed temperature, and the two-site correlation functions for nearest neighbors which give the probability that a nearest neighbor site next to an occupied site is also occupied. They are given as thermal averages, e.g. $\langle n_i^{(e)} n_{i+a}^{(t)} \rangle$, $\langle n_i^{(t)} n_{i+a}^{(t)} \rangle$, $\langle n_i^{(t)} n_{i+a}^{(b)} \rangle$ etc. The deviations from their values for a noninteracting adsorbate, e.g. $\langle n_i^{(e)} n_{i+a}^{(t)} \rangle - \langle n_i^{(e)} \rangle \langle n_{i+a}^{(t)} \rangle$, are a measure for the effectiveness of the lateral interactions.

As the growth curves, Fig. 7d, show adsorption at low coverage is equal for the three sites; at $\theta = 1/3$ a local minimum has developed in the terrace occupation at low temperature ($\theta_t = 0$ at $T = 0$ K and $\theta = 1/3$) for which the e- and b-sites are preferentially occupied since they have the lowest coordination. At $\theta = 1/2$ the e- and b-sites are fully occupied (at low T) and further adsorption into the terrace sites is accompanied by structural re-arrangements. In particular, at $\theta = 2/3$ the occupation of the terrace sites at high temperature which leads to a continuous rise in the t–t correlator, is depleted at low temperature in favor of an

Fig. 6. TPD spectra and equilibrium properties for CO on a model fcc(111) surface with a nearest neighbor repulsion of $V_1^{(t-t)} = 0.1$ eV and $S = (1-\theta)$. Molecular properties (for CO): gas phase $T_{vib} = 3070$ K and $T_{rot} = 2.77$ K; adsorbed phase: $T_{hvib} = 3000$ K and $T_{hrot} = 600$ K; $V_t = 1.46$ eV. Other parameters as in Fig. 2. (a) Desorption rates; (b) heat of adsorption for $T = 200$, 350 and 500 K (top to bottom at $\theta = 0.2$); (c) differential entropy for the same temperatures (bottom to top).

ordered structure which has the six-fold coordinated (interior) t-sites unoccupied leading to a minimum in the t–t correlator at low T, see Fig. 7e. Further information about the process is contained in the heat of adsorption and the differential entropy in Fig. 7f and g. The overall drop in Q_{iso} over the full coverage range must be the same as for the homogeneous surface because the last (terrace) particle added also sees six neighbors. However, at intermediate coverages new structures (sudden variations in Q_{iso} and ΔS) can form due to differing local environments. For example, at $\theta = 1/3$ there is a drop of V_1 in the heat of adsorption when the next particle adsorbs into a terrace site.

We have investigated other terrace widths and the on-top lattice structure and found that adsorption and desorption can be significantly different from the above. There is obviously a variety of phenomena which can be explored for finite systems with approximately homogeneous binding and repulsive lateral interactions.

We now study a more realistic system in which the binding at the three sites is distinct. In Fig. 8 we show adsorption–desorption data for the 7-surface with the differences in the site binding energies being larger than the lateral repulsions and including next nearest neighbor repulsions. This results in a multi-peaked TPD spectra as depicted in Fig. 8a. Again the origin of the various peaks, and the complexity associated with the repulsions, can be observed in the partial rates in Fig. 8b. The highest temperature peak at 570 K is due to desorption of isolated molecules from the e-sites as is part of the desorption around 400 K shifted down by repulsion, in part due to $V_{1s}^{(b-e)}$. (The reason why the highest temperature peak is not around 680 K as in Fig. 2a is due to the fact that for the present molecular desorption the prefactor is larger by about two orders of magnitude (due to the internal modes of CO) from the one for atomic desorption in Fig. 2a.) The b- and the t-sites desorb over a broad temperature range with considerable overlap, again due to the intricate competition between lateral repulsions and the binding energy differences. The finite (negative) rate for the b-sites (amplified by a factor of seven in Fig. 8b) at lowest temperature is due to a transfer of these particles to the e-sites and not due to desorption. This can also be seen in Fig. 8c, as a partial coverage initially increasing with temperature during desorption.

Turning next to the equilibrium properties we first look at the isothermal growth curves in Fig. 8d for temperatures spanning the desorption range. Starting with the clean surface the e-sites become occupied first up to half of their number when the more weakly bound b- and t-sites follow rather linearly with coverage. Above half a monolayer there is a trade-off between the growth on the e- and b-sites. For isothermal desorption these growth curves, followed in reverse from the highest to zero coverage, give the depletion of the various sites as the total coverage decreases. In TPD one follows the partial coverages not along an isotherm but curves that at the highest coverage start at the lowest temperature and then gradually cross over to the highest temperature at the lowest coverage. Further details of the isothermal growth or desorption modes can be gained from the coverage dependence of the correlation functions in Fig. 8e. Not surprisingly the $\langle n_i^{(e)} n_{i+a}^{(b)} \rangle$ correlations build up first because the e-sites are filled first. Although the b- and t-sites grow together initially one can see from the fact that the t–e correlator is always larger than the t–b correlator that the t-sites adjacent to the e-sites are first filled rather than the t-sites adjacent to the b-sites. Because the growth of the t-sites is essentially linear with coverage the corresponding t–t correlator is quadratic in coverage.

As the last equilibrium properties we look at the heat of adsorption (or cum grano salis, the desorption energy) and the differential entropy, see Fig. 8f and g. At the lowest temperature steps are clearly visible in the heat of adsorption which originate either at the appearance of an ordered structure or at the saturation of a particular type of adsorption sites. Thus at coverage 1/14 every second e-site is occupied (at low temperature) and above this coverage an additional particle goes either into the b- or t-sites producing a drop in the isosteric heat due to the binding energy differences. The decrements in the heat of adsorption at higher coverages are again due to the competi-

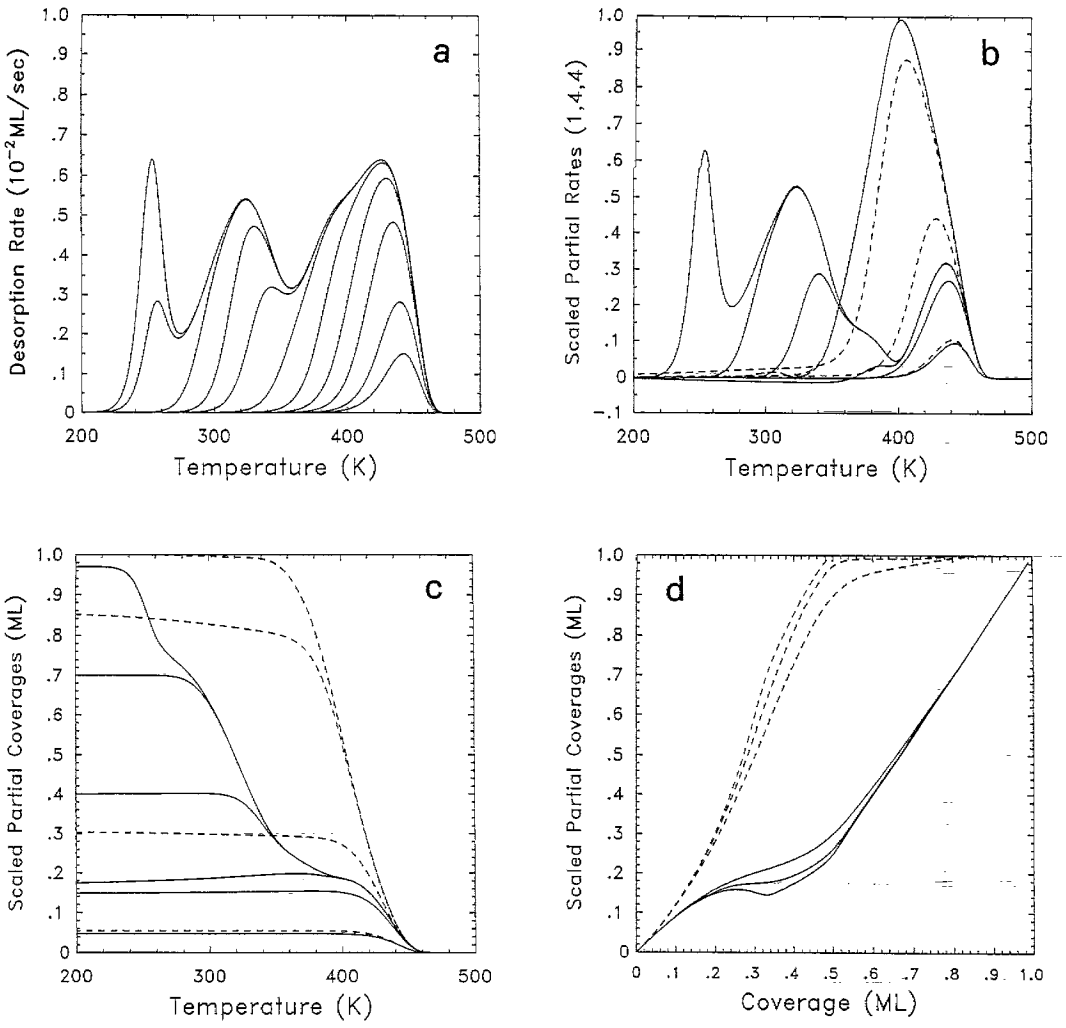

Fig. 7. TPD spectra and equilibrium properties for a molecular adsorbate (CO) on a homogenous 6-surface with parameters as in Fig. 6. (a,b) Total and scaled partial desorption rates (b-sites (dotted lines in previous figures) are equivalent here to e-sites and omitted for clarity). (c) Partial coverage curves as a function of temperature, scaled to site occupations, i.e. $\theta_i m/(m-2)$ (solid lines), $\theta_e m$ (dashed lines), with $m=6$. Only every other initial coverage is plotted. See Eq. (6) also. (d) Isothermal growth curves for $T=$ 200 K (most structured curve), 350 K, 500 K (smoothest curve). Same scaling as in (c). (e) Nearest neighbor correlation functions for same temperatures: ⟨tt⟩ solid, ⟨et⟩=⟨tb⟩ dashed, ⟨eb⟩ long-dashed. (f) Heat of adsorption for 200, 350 and 500 K (top to bottom at $\theta=0.2$). (g) Differential entropy.

tion between the various lateral repulsions. We also show as a dashed line the desorption energy as obtained from an isosteric Arrhenius analysis of the TPD spectra in Fig. 8a [28]. In effect it is a temperature average of the isosteric heat over the temperature range of desorption.

In Fig. 8g we show for completeness the differential entropy for which the details of the coverage dependence is similar to the one given above for an adsorbate on a flat surface, see the discussion of Fig. 6c. Also shown is the prefactor from the Arrhenius analysis which is, of course related to the differential entropy because $\nu_{\text{eff}} \propto \exp(-\Delta S)$. Unlike the differential entropy

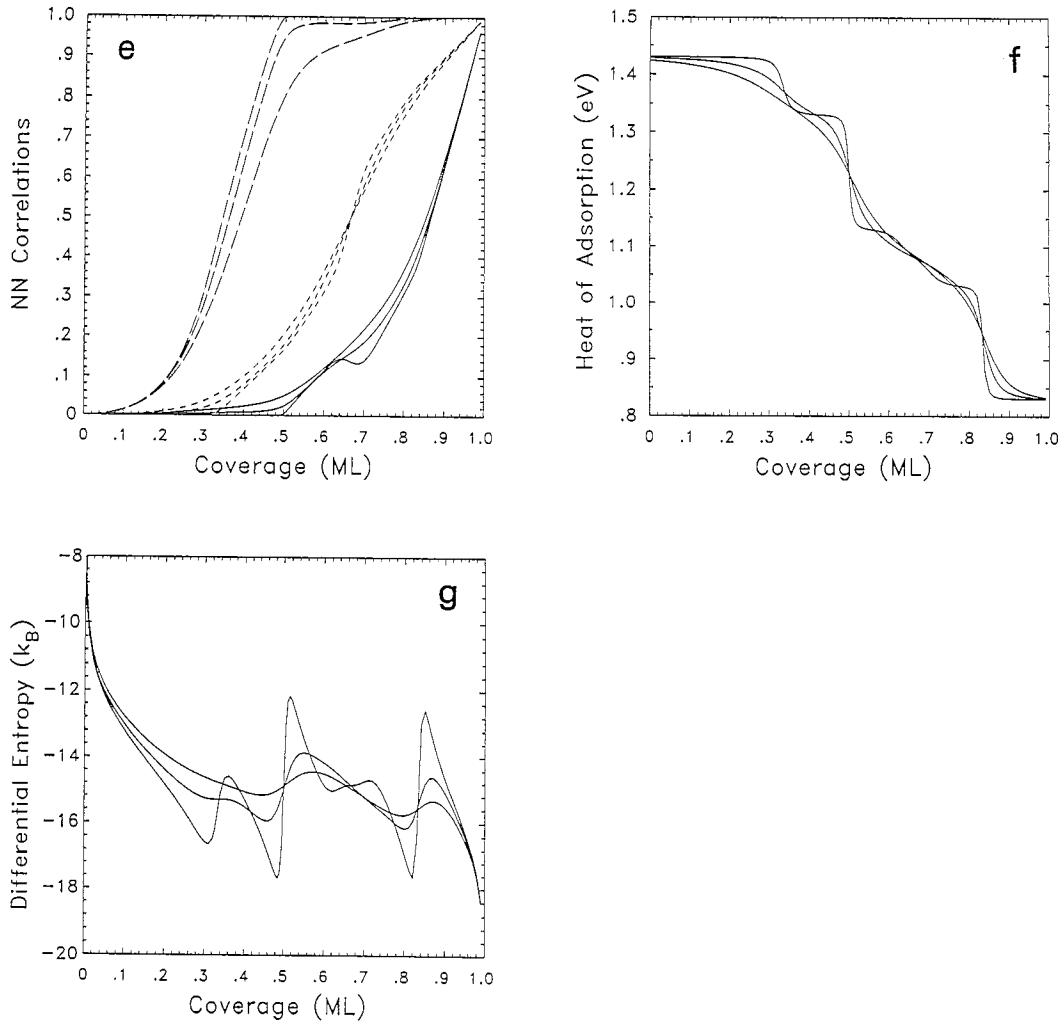

Fig. 7 (*continued*)

the prefactor is not divergent as coverage goes to zero because we have assumed a first-order desorption process ($x=1$) in the Arrhenius parametrization (Eq. (10)).

We now complement this picture of adsorption and desorption on the 7-surface of an adsorbate with strong lateral repulsions with the total and partial desorption rates on the other surfaces of narrower terrace widths. Starting with the surface with b- and e-sites only (i.e. no internal terrace sites at all) the TPD spectra consist of overlapping low and high temperature pairs of double peaks for essentially independent desorption with the double-humped structure in either pair reflecting the strong repulsion along the rows of e- and b-sites, see Fig. 9a–c. However, the overlap results in a mass transfer between these sites as desorption proceeds. On the 3-surface an additional row of t-sites can be occupied between the e- and b-sites, and there is now an additional interplay between the b- and t-sites, due to both binding energy differences and lateral repulsions leading to complicated TPD spectra, and reflected in the growth curves, see Fig. 9d–f. This picture changes as we

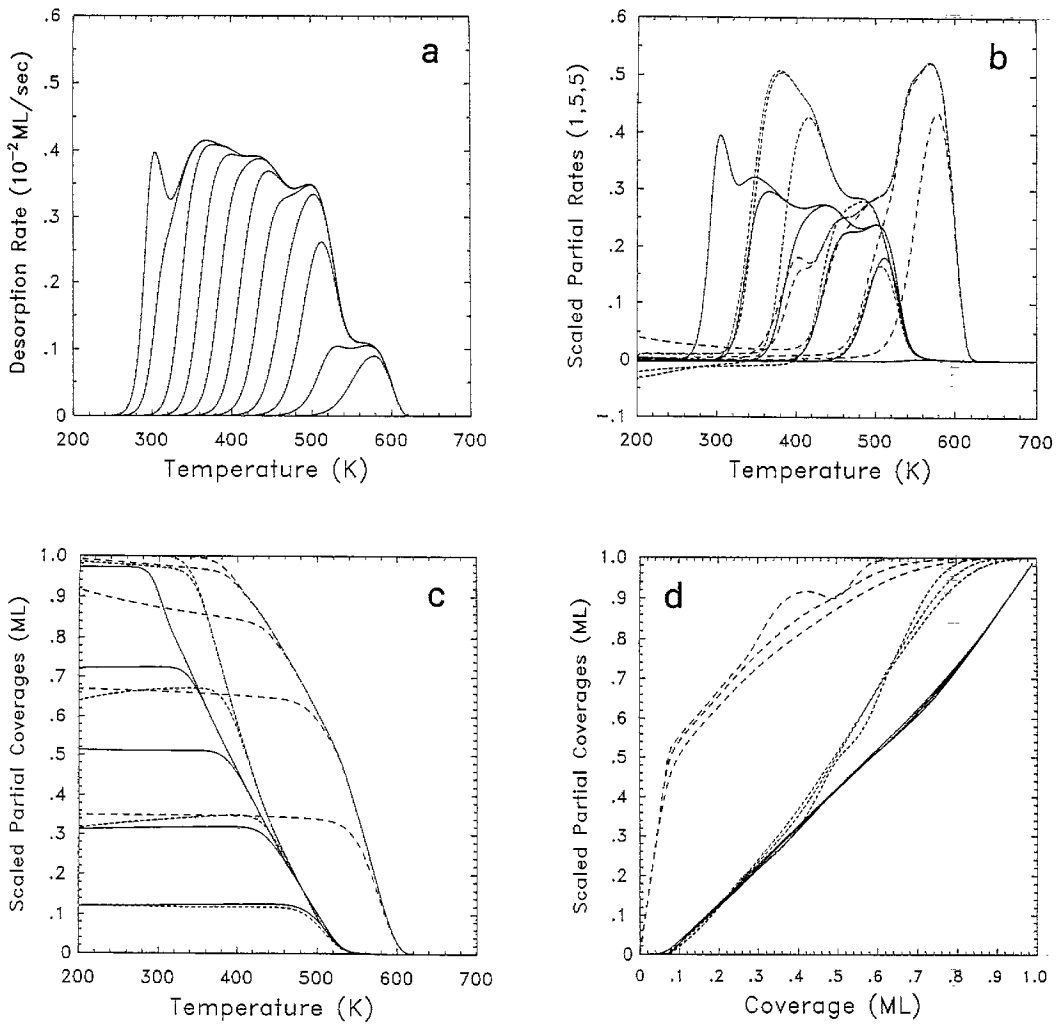

Fig. 8. TPD spectra and equilibrium properties for a molecular adsorbate (CO) on the 7-surface (rotated structure) with parameters: $V_e=2.0$ eV, $V_b=1.8$ eV, $V_t=1.7$ eV, $V_1^{(e-t)}=V_1^{(t-t)}=V_1^{(t-b)}=V_{1s}^{(b-e)}=0.1$ eV, $V_2^{(e-e)}=0.15$ eV, $V_2^{(t-t)}=V_2^{(b-b)}=0.05$ eV, $S=1-\theta$. (a,b) Total and scaled partial desorption rates. (c) Partial coverage curves as a function of temperature, scaled to site occupation. (d) Isothermal growth curves for $T=200$ K (most structured curve), 400 K, 600 K (smoothest curve). Same scaling as in (c). (e) Nearest neighbor correlation functions. ⟨tt⟩ solid, ⟨tb⟩ dotted, ⟨et⟩ dashed, ⟨eb⟩ long-dashed. (f) Heat of adsorption for 200, 400 and 600 K (top to bottom at $\theta=0.2$), solid lines, and desorption energy, dashed line. (g) (Negative of) differential entropy, solid lines, and prefactor, dashed line.

go to the 5-surface where the repulsion between the t-sites sets in, leading to Figs. 9g–i. Observe here that considerable exchange of particles between sites is occurring before any desorption sets in. Although the TPD spectra for $m=3, 5, 7$ are qualitatively similar, the individual site adsorption, hence desorption, processes are noticeably different. Thus, one cannot infer from similar TPD spectra (total rate) alone the equivalence of the adsorption process on different terraces and one needs additional experimental information such as partial coverages.

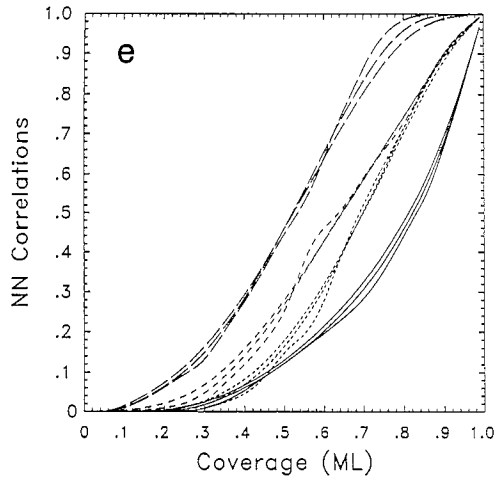

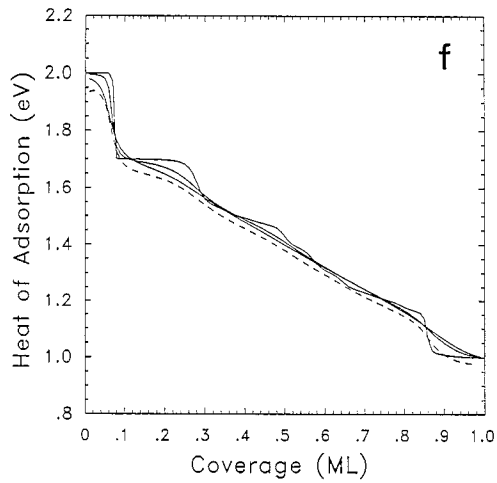

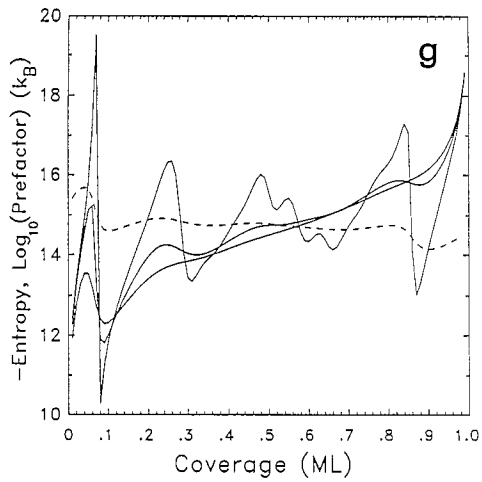

Fig. 8 (*continued*)

7. CO on stepped Pt surfaces

CO adsorption and desorption on stepped surfaces has been investigated thoroughly over many years, see the references in Refs. [29,30]. As on most other surfaces CO on Pt can adsorb in at least two adsorption sites, on-top and bridge-bonded. As an additional complication, there is a re-orientation of the molecular axis on the terrace as well as at the steps as coverage builds up [29]. Although we have incorporated such features in a multi-site, multi-state lattice gas model on a flat surface for other systems [6,31] our present model of stepped surfaces (with on-top adsorption only) does not include these features. Still, this model allows us to reproduce the qualitative features of TPD data for CO on Pt(112) and Pt(335). We have taken the binding energy and the vibrational frequencies on the terrace sites either from experimental data for CO adsorption on Pt(111) or from a fit to TPD spectra on the flat surface [32,33]. In the absence of other information and to keep the number of parameters small we take the same frequencies for all sites on the stepped surfaces.

We model the Pt(112) surface as having three

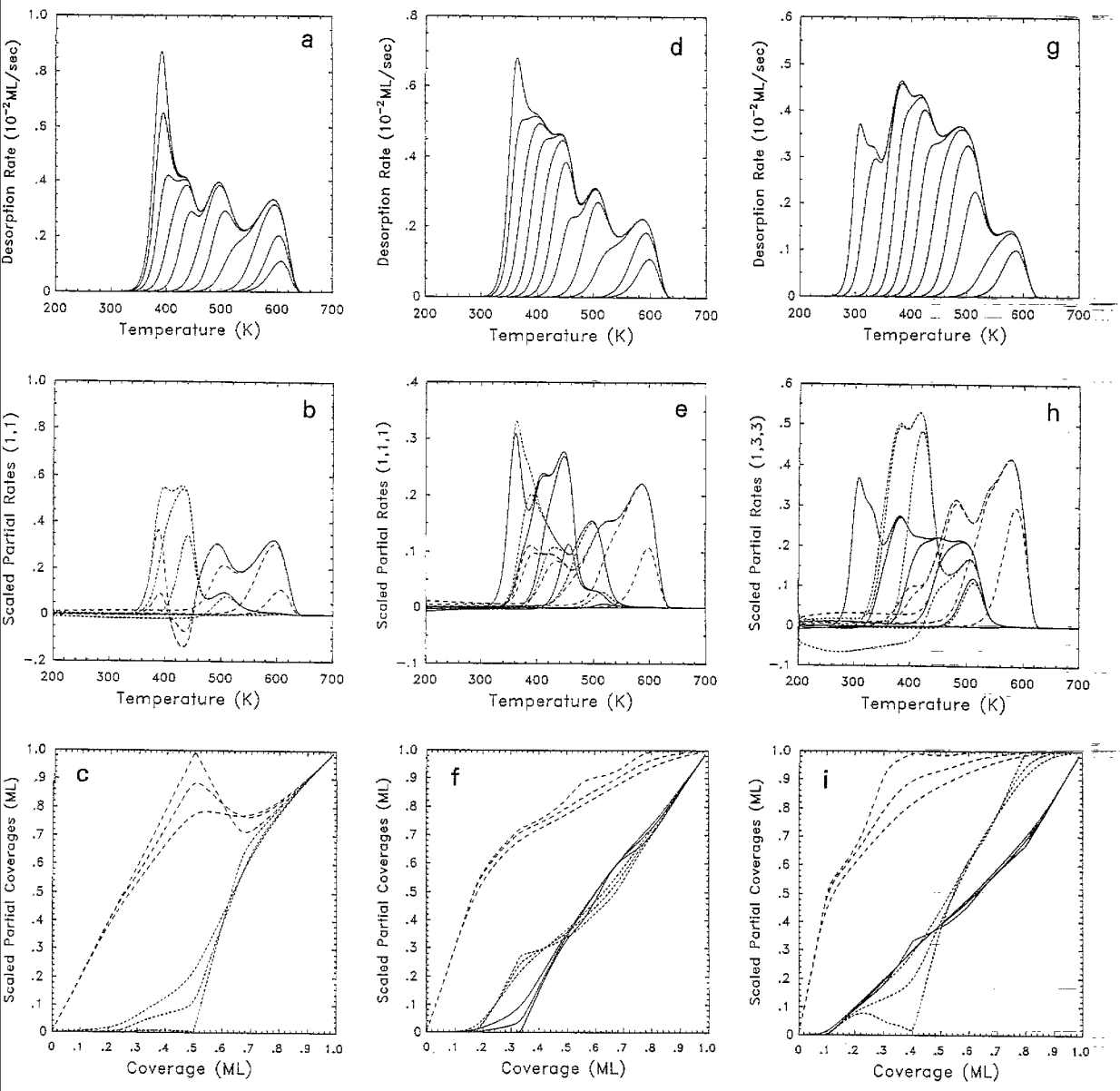

Fig. 9. TPD spectra (total and partial rates) and isothermal growth curves for the system of Fig. 8 but with varying terrace widths. (a–c) 2-surface, (d–f) 3-surface, (g–i) 5-surface.

rows of adsorption sites (e, t and b) for CO. The known ordered structures [29] allow us to assign lateral interactions as follows: there must be a nearest neighbor repulsion, $V_1^{(e-e)}$, along the steps and an even stronger repulsion along the base of the steps, $V_1^{(b-b)}$, to exclude occupation of nearest neighbor b-sites. Binding energy differences and the other lateral interactions are chosen to give a reasonable fit to the experimental TPD data [34]. It is also known that the sticking coefficient is approximately constant up to coverages close to saturation. The resulting TPD spectra are shown in Fig. 10b together with the experimental data in Fig. 10a. The appearance of the low temperature

peak at 0.4 of saturation coverage (curve b in Fig. 10a) is reproduced. Our low temperature peak is not quite wide enough, it is also too high and the valley between the peaks is too deep. We suspect that these deficiencies can be overcome by the introduction of additional binding sites of slightly different energy. However, this is not the point of our exercise here. Rather, we want to show that with the same model parameters and with addition of one more identical terrace sites we can obtain a qualitative fit to TPD data of the Pt(335) surface. This is shown in Fig. 10c and Fig. 10d. Further progress on these systems can only be made with more data, both kinetic and equilibrium, and a detailed model along the lines outlined above.

8. Dissociative adsorption with mainly repulsive interactions

We finally look at dissociative adsorption of homonuclear diatomic molecules assuming that

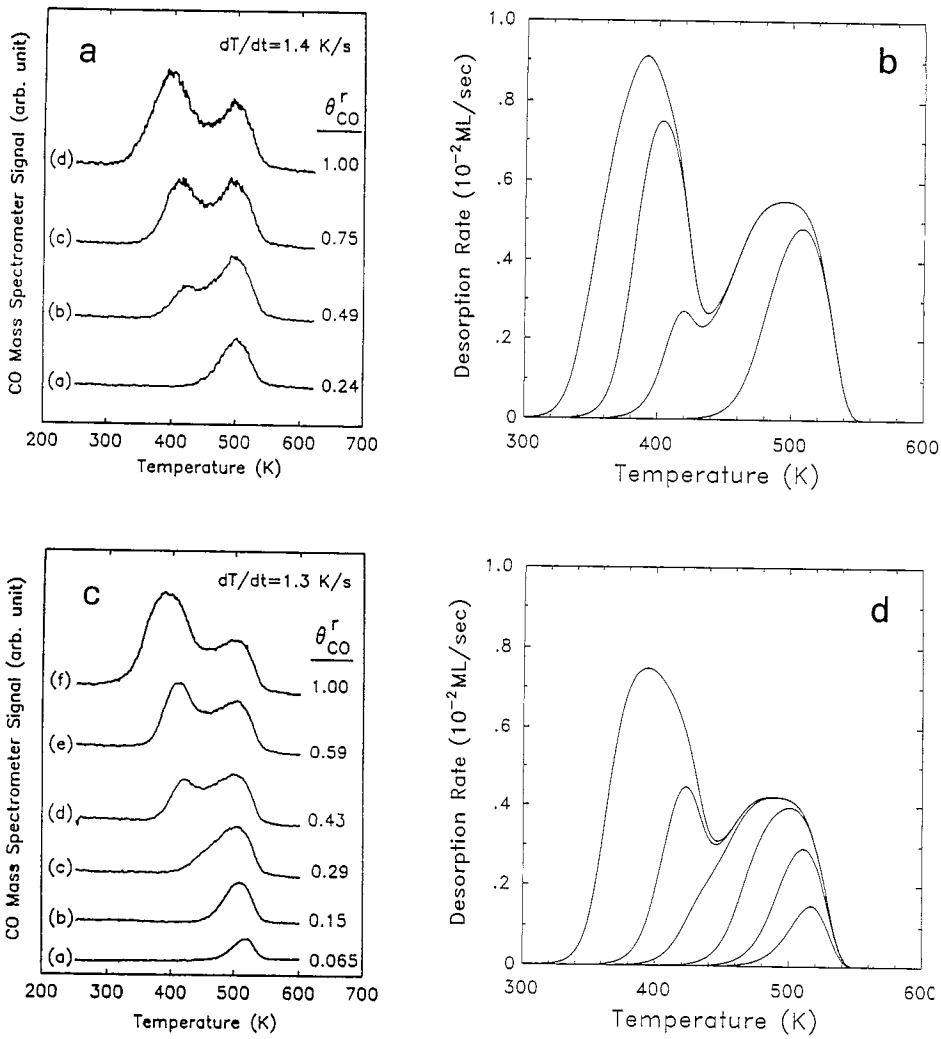

Fig. 10. TPD spectra for CO on stepped Pt. (a) Experimental and (b) theoretical ($m=3$, on-top structure) for Pt(112). (c) Experimental and (d) theoretical ($m=4$, on-top structure) for Pt(553). Experimental data reproduced from Ref. [34].

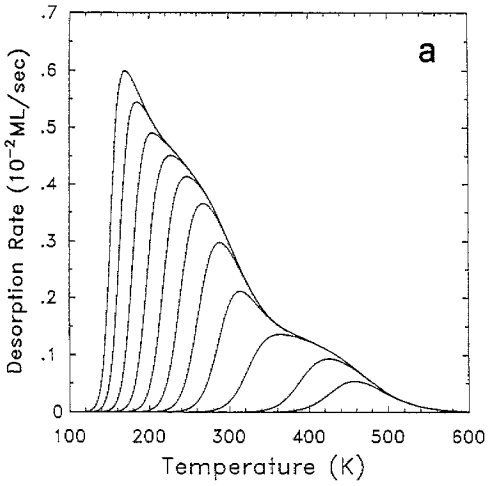
a
Desorption Rate (10^{-2}ML/sec)
Temperature (K)

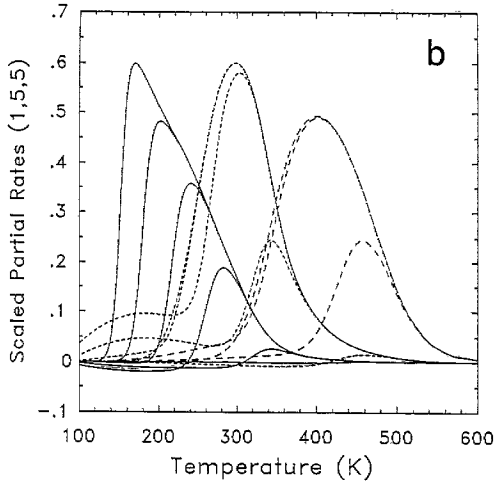
b
Scaled Partial Rates (1,5,5)
Temperature (K)

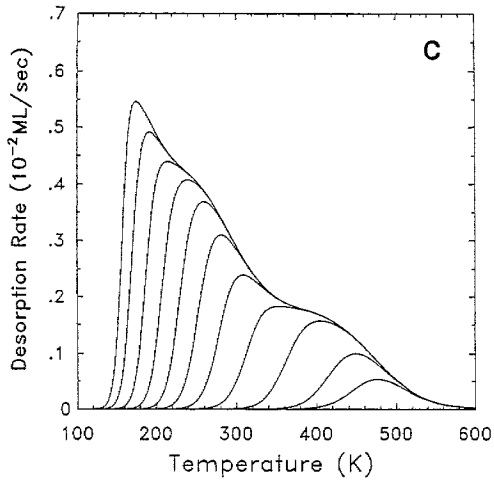
c
Desorption Rate (10^{-2}ML/sec)
Temperature (K)

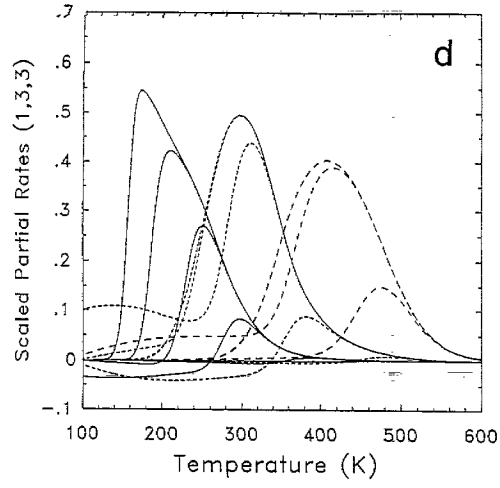
d
Scaled Partial Rates (1,3,3)
Temperature (K)

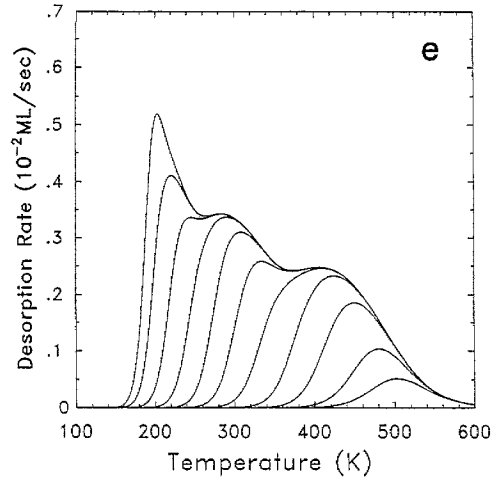
e
Desorption Rate (10^{-2}ML/sec)
Temperature (K)

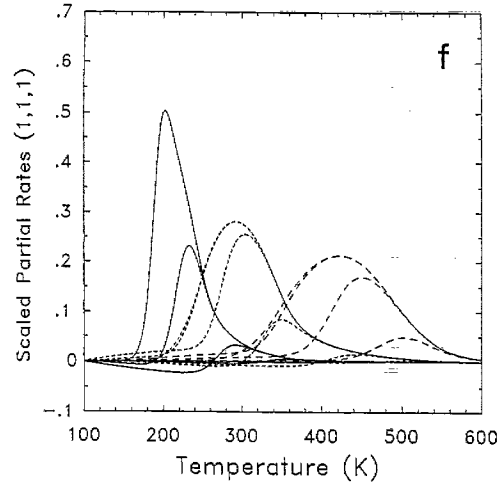
f
Scaled Partial Rates (1,1,1)
Temperature (K)

only atoms are present on the surface. The rate of associative desorption is given by [5]

$$R_{\mathrm{des}} = S(\theta,T)a_{\mathrm{s}} \frac{k_{\mathrm{B}}T}{h\lambda^2(q_3^{(\mathrm{t})})^2} Z_{\mathrm{vr}}\, \mathrm{e}^{-2V_{\mathrm{t}}/k_{\mathrm{B}}T+\epsilon_{\mathrm{dis}}} \times \frac{\theta^2}{(1-\theta)^2}\, \mathrm{e}^{2\mu_{\mathrm{i}}(\theta,T)/k_{\mathrm{B}}T}. \quad (12)$$

Here ϵ_{dis} is the electronic dissociation energy of the gas phase molecule.

For our numerical examples we choose binding energies and lateral interactions appropriate for hydrogen on Pt surfaces [35] without attempting detailed fits. The site binding energy differences are actually the same as those for Fig. 2. Starting with the 7-surface in Fig. 11a and b we note that the main peak has the characteristic features of second-order desorption from the fcc(111) surface with a common trailing edge in this case extended to higher temperatures by desorption from the more strongly bound e- and b-sites as demonstrated by the partial rates. Indeed, desorption from each site has this characteristic because of the weak repulsion. There is some mass transfer between the various sites depending on the initial coverage. Reducing the terrace width to 5 sites (Figs. 11c and d) produces similar total TPD spectra, but the transfer is noticeably increased. For the 3-surface the desorption obviously approximates those of three independent sites with some overlap.

9. Summary and outlook

We have presented a theory of adsorption and thermal desorption of atoms and molecules on stepped surfaces. A lattice gas model has been formulated with different adsorption sites on the terraces, the lower base and the upper edge of the steps and including various lateral interactions. Using transfer matrix techniques we can calculate, accurately, the equilibrium properties, correlation functions and temperature-programmed desorption spectra. A systematic study has been presented on the effect of varying terrace widths for atomic, molecular and dissociative adsorption with attractive and/or repulsive lateral interactions. We have also presented preliminary fits to experimental data on Xe, CO and hydrogen desorption from stepped Pt(111) surfaces.

There are a number of possible extensions of this work that should be undertaken:

(1) When dealing with thermal desorption we have in this paper assumed that fast surface diffusion maintains the adsorbate in quasi-equilibrium over the temperature range of desorption. If this is not the case, e.g. due to limited diffusion across the steps, one must extend the theory to include nonequilibrium effects. This can be done in a kinetic lattice gas model as shown elsewhere for flat surfaces.

(2) So far we have assumed only one kind of adsorption state for step and terrace sites. As we have done elsewhere for flat surfaces, the formalism can easily be extended to include different adsorption geometries, e.g. on-top and bridge sites [6,31]. Similarly, it can be extended to describe multilayer growth, e.g. as observed for Xe adsorption on Pt(997) [26] and on Pd(810) [36]. This has been done already for flat surfaces [37–39].

(3) In this paper we have assumed simple sticking coefficients, either constant or due to site exclusion only. There is enough experimental evidence that on stepped surfaces the steps play a major role in enhancing sticking, in particular dissociative sticking [35]. Such phenomena can again be dealt with in a kinetic lattice gas model [17,40]. In a preliminary investigation we have, as an example, been able to show that the exponential decay of the sticking probability as a function of coverage for hydrogen on Pt(111) and Pt(997) is the result of lateral repulsions as it was the case for oxygen on Ag(100) [40]. The overall

Fig. 11. TPD spectra (total and partial rates) for dissociative adsorption of hydrogen on a metal surface with varying terrace widths. $V_{\mathrm{e}}=3.0$ eV, $V_{\mathrm{b}}=2.9$ eV, $V_{\mathrm{t}}=2.9$ eV, $V_1^{(\mathrm{e-t})}=V_1^{(\mathrm{t-t})}=V_1^{(\mathrm{t-b})}=V_{1\mathrm{s}}^{(\mathrm{b-e})}=V_2^{(\mathrm{e-e})}=V_2^{(\mathrm{t-t})}=V_2^{(\mathrm{b-b})}=0.017$ eV, $S=(1-\theta)^2$. Gas phase parameters: $\epsilon_{\mathrm{dis}}=5.3$ eV, $T_{\mathrm{vib}}=6324$ K, $T_{\mathrm{rot}}=87.5$ K. (a,b) $m=7$, (c,d) $m=5$, (e,f) $m=3$.

increase of sticking on the stepped Pt surface is explained by the higher dissociation probability at the steps.

(4) With the overall theory in place one should now turn to specific examples as we have done, in exploratory fashion, for Xe and CO adsorption on stepped Pt surfaces, and fit experimental data on a series of stepped surfaces. To do this accurately and meaningfully one needs good TPD data, structural information and also equilibrium data to assign unique values to the various binding and interaction energies and vibrational frequencies. There is also evidence now that such microscopic parameters may be extracted from ab initio calculations as it was recently done for oxygen on Ru(001) [41].

Acknowledgements

This work was supported by a grant from the Office of Naval Research.

Appendix A

In this appendix we elaborate on the discussion in Section 3 that even for an adsorbate with negligible lateral interactions the TPD spectra from a stepped surface are not simply the superposition of several independent peaks arising from the different binding sites except when these peaks are well separated in temperature or completely overlap. We consider a slightly simpler system, namely one where the t- and b-sites are energetically equivalent and we assume that there are n_t rows of those plus one additional row of e-sites per terrace. For N_x terraces, each with n_t+1 sites perpendicular to the steps, and N_y sites in the direction parallel to the steps we have a total of $N_s=(n_t+1)N_xN_y$ sites on the surface. The grand potential can then be written as

$$\Omega(T,N_s,\mu)=-\frac{N_s}{n_t+1}k_BT\ln(\xi), \tag{A1}$$

where the partition function for a row of n_t+1 adsorbed particles (perpendicular to the steps) is

$$\xi=\{1+\exp[-(E_t-\mu_t)/k_BT]\}^{n_t}\times\{1+\exp[-(E_e-\mu_e)/k_BT]\}, \tag{A2}$$

where we temporarily introduced different chemical potentials for the e- and t-sites which in equilibrium will be set equal. Differentiation of Eq. (A1) with respect to μ_t and μ_e gives, respectively, the partial coverages of t- and e-sites, namely

$$\theta_t=\frac{n_t}{n_t+1}\{\exp[(E_t-\mu)/k_BT]+1\}^{-1}, \tag{A3}$$

$$\theta_e=\frac{1}{n_t+1}\{\exp[(E_e-\mu)/k_BT]+1\}^{-1}, \tag{A4}$$

from which one can get the chemical potential, $\mu=\mu_t=\mu_e$, as a function of $\theta=\theta_t+\theta_e$ and T (by solving a quadratic equation) as

$$e^{\mu/k_BT}=\frac{b}{2(1-\theta)}[1+(1+4(1-\theta)\theta\times\exp((E_t+E_e)k_BT)b^2)^{1/2}], \tag{A5}$$

where

$$b=[\exp(E_t/k_BT)+\exp(E_e/k_BT)]\theta-\frac{1}{n_t+1}\exp(E_t/k_BT)-\frac{n_t}{n_t+1}\exp(E_e/k_BT). \tag{A6}$$

For the partial rate of desorption from the terrace sites we find (using Eq. (A3))

$$\frac{d\theta_t}{dt}|_{des}=-S_t(\theta_t,T)a_s\frac{k_BT}{h\lambda^2}\exp(\mu_t/k_BT)=-S_t(\theta_t,T)a_s\frac{k_BT}{h\lambda^2q_3^{(t)}}e^{-V_t/k_BT}\theta_t\frac{n_t+1}{n_t}\times[1+\exp(-E_t/k_BT)\exp(\mu/k_BT)]. \tag{A7}$$

For widely different binding energies for the t- and e-sites, i.e. for $E_t\gg E_e$, this reduces to

$$\frac{d\theta_t}{dt}|_{des}=-S_t(\theta_t,T)a_s\frac{k_BT}{h\lambda^2q_3^{(t)}}e^{-V_t/k_BT}\theta_t\frac{n_t+1}{n_t}\frac{1}{1-\theta}. \tag{A8}$$

Because for a noninteracting adsorbate the only coverage dependence in the sticking coefficient is due to site exclusion leading to $S_t = S_{t0}(1-\theta_t)$ we see that Eq. (A8) is nothing but the first-order desorption from the independent t-sites without any interference from the desorption at higher temperatures from the much more tightly bound e-sites. If the t- and e-sites are not energetically quite different then they both contribute to the chemical potential in the temperature range of desorption and the total TPD spectrum is no longer the superposition of two independent peaks, as shown in Figs. 2 and 3 in numerical examples.

References

[1] K. Wandelt, Surf. Sci. 251/252 (1991) 387.
[2] P. Hollins, Surf. Sci. Rep. 16 (1992) 51.
[3] K. Wandelt, in: R. Vanselow, R. Howe (Eds.), Physics and Chemistry of Solid Surfaces VIII, Springer, Berlin, 1990.
[4] H. Wagner, in: Springer Tracts in Modern Physics, vol. 85, Springer–Verlag, Berlin, 1979.
[5] H.J. Kreuzer, S.H. Payne, in: W. Rudzinski, W.A. Steele, G. Zgrablich (Eds.), Equilibrium and Dynamics of Gas Adsorption on Heterogeneous Solid Surfaces, Elsevier, Amsterdam, 1997.
[6] H.J. Kreuzer, Z. Jun, S.H. Payne, W. Nichtl-Pecher, L. Hammer, K. Müller, Surf. Sci. 303 (1994) 1.
[7] C. Uebing, R. Gomer, Surf. Sci. 306 (1994) 419.
[8] C. Uebing, R. Gomer, Surf. Sci. 306 (1994) 427.
[9] C. Uebing, R. Gomer, Surf. Sci. 317 (1994) 165.
[10] H.J. Kreuzer, S.H. Payne, Surf. Sci. 200 (1988) L433.
[11] S.H. Payne, J. Zhang, H.J. Kreuzer, Surf. Sci. 264 (10) (1992) 185.
[12] F.H. Ree, D.A. Chesnut, J. Chem. Phys. 45 (1966) 3983.
[13] L.D. Roelofs, R.J. Bellon, Surf. Sci. 223 (1989) 585.
[14] N.C. Bartelt, T.L. Einstein, L.D. Roelofs, Phys. Rev. B 34 (1986) 1616.
[15] P.A. Rikvold, K. Kaski, J.D. Gunton, M.C. Yalabik, Phys. Rev. B 29 (1984) 6285.
[16] S.H. Payne, H.J. Kreuzer, L.D. Roelofs, Surf. Sci. 259 (1991) L781.
[17] H.J. Kreuzer, J. Chem. Phys. 104 (1996) 9593.
[18] C. Benndorf, L. Meyer, J. Vac. Sci. Technol. A 8 (1990) 2677.
[19] E.V. Albano, K. Binder, D.W. Herrmann, W. Paul, Surf. Sci. 223 (1989) 151.
[20] E.V. Albano, K. Binder, D.W. Herrmann, W. Paul, J. Chem. Phys. 91 (1989) 3700.
[21] E.V. Albano, K. Binder, D.W. Herrmann, W. Paul, Z. Phys. B 77 (1989) 445.
[22] J. Merikovski, J. Timonen, K. Kaski, Phys. Rev. B 50 (1994) 7925.
[23] U. Bardi, A. Glachant, M. Bienfait, Surf. Sci. 97 (1980) 137.
[24] C.T. Rettner, D.S. Bethune, E.K. Schweizer, J. Chem. Phys. 92 (1990) 1442.
[25] H.R. Siddiqui, P.J. Chen, X. Guo, J.T. Yates Jr., J. Chem. Phys. 92 (1990) 7690.
[26] W. Widdra, P. Trischberger, D. Menzel, S.H. Payne, H.J. Kreuzer, to be published.
[27] H. Pfnür, D. Menzel, J. Chem. Phys. 79 (1983) 2400.
[28] The analysis of the data and some of the modeling were performed with the ASTEK package written by H.J. Kreuzer and S.H. Payne (available from Helix Science Applications, Box 49, Site 3, R.R. 5, Armdale, NS, Canada B3L 4J5).
[29] M.A. Henderson, A. Szabo, J.T. Yates Jr., J. Chem. Phys. 91 (1989) 7245.
[30] J.D. Batteas, D.E. Gardin, M.A. van Hove, G.A. Somorjai, Surf. Sci. 297 (1993) 11.
[31] H.J. Kreuzer, S.H. Payne, M. Grunze, Ch. Woell, Z. Phys. Chem. to be published.
[32] H. Steininger, S. Lehwald, H. Ibach, Surf. Sci. 123 (1982) 264.
[33] G. Hähner, J.P. Toennies, Ch. Wöll, Appl. Phys. A 51 (1990) 208.
[34] Jiazhan Xu, J.T. Yates Jr., Surf. Sci. 327 (1995) 193.
[35] K. Christmann, G. Ertl, Surf. Sci. 60 (1976) 365.
[36] R. Miranda, S. Daiser, K. Wandelt, G. Ertl, Surf. Sci. 131 (1983) 61.
[37] S.H. Payne, H.J. Kreuzer, Surf. Sci. 338 (1995) 261.
[38] S.H. Payne, H.J. Kreuzer, A. Pavlovska, E. Bauer, Surf. Sci. 345 (1996) L1.
[39] S.H. Payne, H.A. McKay, H.J. Kreuzer, M. Gierer, H. Bludau, H. Over, G. Ertl, Phys. Rev. B 54 (1996) 5073.
[40] F. Buatier de Mongeot, M. Rocca, A. Cupolillo, U. Valbusa, H.J. Kreuzer, S.H. Payne, J. Chem. Phys. 106 (1997) 711.
[41] C. Stampfl, M. Scheffler, H.J. Kreuzer, in preparation.